UNIVERSITATEA DIN BUCUREȘTI
VIRTUTE ET SAPIENTIA

UNIVERSITY OF BUCHAREST

The Faculty of Geology And Geophysics

FACULTATEA DE GEOLOGIE ȘI GEOFIZICĂ, UNIVERSITATEA DIN BUCUREȘTI

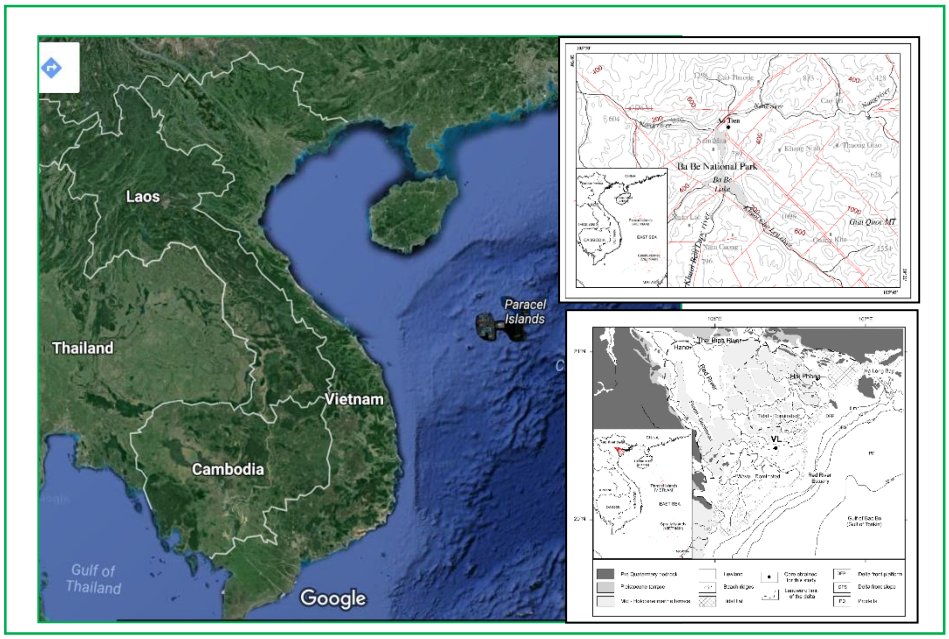

SUMMARY THESIS

RECONSTRUCTING AND CHARACTERISING THE HOLOCENE PALEOCLIMATE AND PALEOENVIRONMENT FROM SEDIMENTS IN NORTHERN VIETNAM

- A CASE STUDY RED RIVER DELTA AND BA BE LAKE -

Supervisor

Prof. Dr. Gheorghe C. POPESCU

PhD student

Hoang Van Tuan

Bucharest, 2019

TABLE OF CONTENTS

CHAPTER 1. GENERAL INTRODUCTION

1.1. The climate of the Holocene

The climate of Holocene has been an important role in the growth and development of modern society, but the knowledge about climate change during this time was limited. Decades of paleoclimate studies show the frequency of extreme climatic events along with the last glacial maximum (LGM). Reconstruction of paleoclimate changes is important not only for understanding the character of the climate features and human activities are impacting the climate system, but also providing a data systems support to run global climate models which in great detail and high accuracy (Berger, et al., 2012). The studies show the change in the spatial and seasonal incoming solar radiation by the quasi-cyclic variations in the Earth's orbit and the major cause of global climate variability is solar radiation.

Holocene climate research has achieved a key role in producing wealthy data on the variation of natural climate change since the LGM. Pioneering Holocene climate research based on investigation about macrofossils, megafossils, and peat stratigraphy of pine trees which conserved in peat (Scandinavia). Heinrich Dau (1829) became the first scientist, who studied the Holocene climate changes though peat. He investigated the presence of pinewoods in peat and the stratigraphic changes due to their type and color. Moreover, he tried to explain the presence of pine megafossils as reflecting a phase during the hypothetical forest history of Denmark. However, he did not have a chance to test his hypothesis.

During 20 years, the main conflict between the Andersson's approach and the Blytt-Sernander scheme. In 1946, Lennart von Post showed that the history of the post-glacial climate has been affected by both precipitation change (Blytt-Sernander scheme) and temperature changes (Andersson's approach). This proposal would have developed together with the improvement of pollen analysis.

Although the limitations of the various techniques available, the results of the study by Steentrup, Vaupell, Dau, Praeger, Jamieson, Sernander, Blytt, and Brøgger were very remarkable. However, these results were largely pretermitted until the improvement of pollen analysis which as a tool for reconstructing past climates during the Holocene. Until the 1970s, the studies of peat stratigraphy in Scandinavia were inspirited by new techniques, which have been used for detecting changes in bog moisture (testate amoebae), evaluating peat humification and calculating chronologies (radiocarbon dating) (Aaby, 1976, Aaby&Tauber, 1975).

In 1916, Lennart von Post presented and suggested the potential applicability of technique which has been used to determine relative dating and reconstruct past vegetation and past climate. He introduced the term "regional parallelism", meaning that the Holocene climatic optimum can be reflected in various ways across diverse taxa in various climatic regions and geographic regions. He also had the vision of pollen stratigraphy, it's soon become the only approach used to detect past climate changes and to classify the Blytt - Sernander periods. Between the period 1920s and 1940, many publications conducted with pollen analysis studies in Europe, China, North America, South America, and New Zealand (Battarbee&Binney, 2009).Moreover, he showed that pollen analysis studies in several areas on the Earth (North America, Chile, Japan,...), to identify the various climate along the Holocene with the circulation systems of the Earth. Between the period 1940s and 1960s, the main advances in methods of pollen analysis were conducted by Johs. Iversen, Knut Fægri, and other scientists. In 1944, according to the study of fossil pollen which appeared in Holocene sediments (southern Scandinavia), Iversen suggested that summer and winter seasons during the middle Holocene could be warmer than today. After, Iversen's analysis was accepted by Walther et al. (2005). He investigated that the northern margin (in Scandinavian) was transformed in the past 50 years in response to climate changes recently. While there was evidence for the effects of human activity which resulted in changing land use conditions concerning climate change.

Until the 1970s, Holocene climate researcher had collected a large volumes of pollen-stratigraphic and other data (radiocarbon dating), which has been provided an independent chronology (Battarbee&Binney, 2009). Reconstruction of paleoclimate and paleoenvironment have been used these data, they were mainly qualitative and according to indicator species or a comparative approach (visually comparison of the fossil and modern assemblages).

The international Cooperative Holocene Mapping Project (COHMAP) started in 1977 for climate changes along the Holocene. Paleoclimate modelers were built with pollen data and it rapidly achieved widespread popularity. Comparison between the results calculated which used to the Community Climate Model (CCM) for simulating past climates at 18000, 15000, 12000, 9000, 6000, 3000, and 0 years before the present and the various paleoclimate data sources, lake-level data, marine plankton data, and particularly terrestrial pollen data (Wright, 1993). COHMAP was showed a large improvement in Holocene climate research. This model has been used in the state of climate models that reproduced the past climate variability under the conditions of specified boundary layers. Moreover, this model also was described in detail for syntheses and compilations of paleoclimate proxy data which have been used to compare data modelling. It was understood the climate system in the world and reviewed the strong regional correlation between various constituents of the Earth's

climate system. Furthermore, it revealed remarkable of the circulation patterns of the Earth's climate process change over time.

Although Holocene climate research has been made advances by reconstructing the Holocene climate evolution over the past 200 years, it also has several problems that relate to data interpretation, dating, data collected, and limitations of our understanding (Battarbee&Binney, 2009).

1.2. Climate forcing factors during the Holocene

Climate is identified as a region's weather patterns which include humidity, temperature, atmospheric pressure, and another meteorological variability in a long time. Thus, the climate is determined by the average weather in the location over long periods. Several external forcing factors impacted on the Holocene climate changes, including solar variability, orbital forcing, and volcanic forcing. In fact, all of these factors interacted with each other and they also impacted on the Earth's climate system. Moreover, the role of human activities based on determining vegetation cover and land-use changes, which effected climate change along the Holocene.

During the Holocene, solar irradiance has been changed due to different latitudes. In the late Holocene (about 6 cal, kyr BP), solar irradiance was more influential than the present time. In the early Holocene, the gradual influenced by external forcing drives the Earth's climate system and it caused by abrupt climate change and occurred similar in several areas of the World, however, these variations are not immediately apparent. In the Northern Hemisphere, for instance, the ice melts slowly and sea-level rise steadily. Thus, sea-level could middle Holocene sea-level after some millenials. Similarly, species evolve too slowly to adapt to global warming during the Holocene. The processes of migration, completion, and evolution, which are contributed to changing the surface of the Earth.

The main factor that impacted to Holocene climate changes and related to three orbital parameters including obliquity, precession, and eccentricity. Although these parameters have a low affected on the total volume of solar radiation released by the Sun, however, they are strongly influenced by solar radiation variation on different seasons and latitudes. Precessional shifts due to perihelion at the time which occurred only during the summer in the North of Hemisphere along the early Holocene. Therefore, daily insolation values at various latitudes (northern hemisphere) in the summer are higher than others (values from ~40 °W/m^2 higher than present at 60 °N to 25 °W/m^2 higher at the Equator). Besides, July insolation has slightly decreased over the 12 kyr before our time. While thermal anomalies were generally smaller during summer in the South of Hemisphere and it normally located at lower latitude (Mackay, et al., 2003).

Orbital forcing effects on the distribution of incoming solar energy following attitudinally and seasonally. Therefore, it could be various responses to the forcing in the southern and northern hemispheres of the Earth which impacts the global climate system. Although the variation of solar irradiance could be influenced similar to all parts of the Earth, the amplification of solar radiation was not effected for all regions, caused by interaction and feedbacks in the atmosphere of the Earth (Rind, 2002).

Volcanic activities are the major caused of strong short-term cooling, because the injection of large volume of gases (CO_2, H_2O, SO_2, N_2) and dust into the atmosphere disarranges reducing energy receipts at the surface of the Earth. The variation of atmospheric circulation made some temperature anomalies somewhere which means climate in somewhere was cool and others are warm. The climate over the mainland was warm during wintertime (in high altitude areas), caused mainly by volcano eruptions in the 20th century.

Along the Holocene, environment systems have influence by the different economic development activities as building and agriculture. Impacts of human activities on creating and changing the environmental systems which showed through the changing of land-use. These effects consisted of feedbacks on the Earth's climate system, both direct and indirect, through changes in atmosphere gases (Battarbee&Binney, 2009). Impact of human activities on weather and climate associated with the appearance of mankind. It was closely related to the fate of past cultures and civilizations in the long term. The nature of the social organization, its flexibility, and adaptive capacity are important in determining human in this society could be survivable and developing or extinct during Holocene (Battarbee&Binney, 2009).

1.3. Climate variability during Holocene in the world

According to the results study base on the GISP2 Greenland ice core, Denton and Kalén (1973) investigated that the Holocene glacial record could be classified as 9-8, 6-5, 4.2-3.8, 3.5-2.5, 1.2-1, and 0.6-1.5 cal. kyr BP (Denton&Karlén, 1973, Martin, et al., 2007, Mayewski, et al., 2004).

The feature of this period was severe climatic disruption and it was unique among rapid climate change (RCC) intervals along the Holocene, caused by this period occurred at a time when large in North of Hemisphere ice sheets were still at the moment. In the Atlantic, an abrupt climate event 8.2 kyr before present brought generally dry and cold climatic conditions (the "8k" event). The occurrence of ice rafting, strengthened atmospheric circulation over the Siberia and North Atlantic which showed considerably cooler temperatures than others and increased the frequency of outbreaks of cold air from the northeast over the Aegean Sea (Mayewski, et al., 1997, Rohling, et al., 2002). In

the European Alps, the occurrence of glacier retreat suggested the impact of dry northerly winds in the Northern Hemisphere (Hormes, et al., 2001). In additional support to this hypothesis comes from northwestern North America and Scandinavia where mountain glacier advances occur and treeline limit was lower in Sweden.

Following the period between 9-8 cal. kyr BP, RCC interval occurs with varied geographic extent and it was characterized by low latitude aridity and high latitude cooling (Mayewski, et al., 2004). The most extensive of these reorganizations appeared from 6-5 to 3.5-2.5 cal. kyr BP, with less widespread events appearing at 4.2-3.8 cal. kyr BP and 1.2-1cal. kyr BP.

Although evidences for the RCC interval between 4.2-3.8 and 1.2-1 cal. kyr BP appears in fewer of the record, however, they are characterized by the apparent synchrony and large spatial distributions. Those record also contains evidence which suggested global scale teleconnections as for the other intervals (Mayewski, et al., 2004). In the North of Hemisphere, the westerly winds across the Siberia and North Atlantic were weak, the temperature fell in western North America during this RCC interval (Scuderi, 1993). Although other climatic disruptions, those records generally are synchronous, distributed in a wide range, signs, and intensities (Mayewski, et al., 2004). Some evidence as during the interval 4.2-3.8 cal. kyr BP, mountain glacier advance in North America, but retreat in Euro, while Scandinavian ice showed weakness influencing. Moreover, North Atlantic Deep Water production was low from 4.2-3.8 cal. kyr BP, however, it increased during the 1.2-1 cal. kyr BP (Mayewski, et al., 2004).

In this rapid climate change interval, the polar climate regions (both polars) were a windy and cold climatic condition, however, the aridity conditions at the low latitude that predominated during the earlier of this interval and it does not generally climatic condition the tropic of the most recent interval. Moreover, the missing of some records was occurred during recent sections, caused by artifacts of sampling and anthropogenic influences (Mayewski, et al., 2004). Thus, this event in this study only from 0.6 to 0.15 cal. kyr BP.

1.4. The objective of thesis

Reconstructing and characterizing the environmental changes during Holocene in the North of Vietnam, supply base science for assessment and prediction climate change and environment, to enhance the effectiveness of programs to respond and adapt to climate change and extreme weather phenomena, which are increasingly complex movements.

CHAPTER 2. STUDY AREAS LOCATION AND STATE OF THE ART

2.1. Red River Delta (Vietnam)

The RRD, situated in the western coastal zone of the Gulf of Bac Bo (East Sea, Vietnam), is one of five largest deltas in Southeast Asia in term of delta plain area (approximately 160,000 km^2), after the Chao Phraya, Irrawaddy and Mekong (Li, et al., 2006, Tanabe, et al., 2006). The dominance of the catchment area covers parts of Northern Vietnam and its sediment and water discharge greatly controlled by the hydrological conditions in the Gulf of Bac Bo.

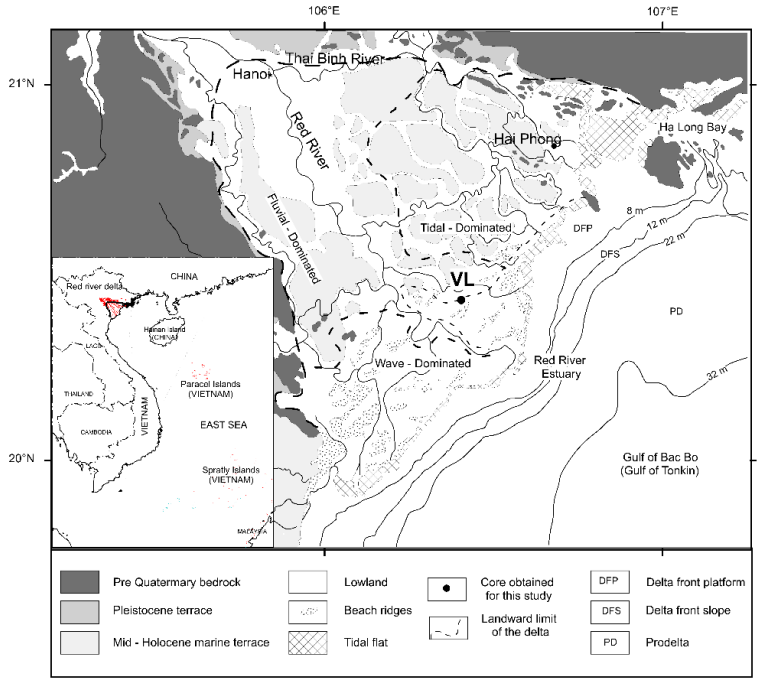

Figure 2.1. Quaternary geology and topography of the Red River Delta, Vietnam (modified from Tanabe et al., (2006))

2.2.1. Geographical setting

The Red River plain has been classified into three subsystems (fluvial-dominated, tide-dominated, and wave-dominated) based upon hydraulic processes and surface topography (Mathers&Zalasiewicz, 1999). The fluvial-dominated subsystem, located in the western part of the delta where the fluvial flux was relatively stronger than others and is consisted of fluvial terraces, flood plain, meandering rivers, and meandering levee belts. The wave-dominated subsystem is characterized by alternating beach ridges and inter-ridge marshes, which spread in the southwestern area of the delta, where wave energy is enhanced due to strong summer monsoon. Besides, the tide-dominated subsystem comprised of tidal flats, marshes, and tidal creeks/channels and is situated in the northeastern part of the delta, where the coast is protected by Hainan island from high energy-waves (Mathers&Zalasiewicz, 1999, Tanabe, et al., 2006).

2.2.2. Geological setting

The Red River plain is covered by mountainous areas, which consisted of Precambrian crystalline rocks as well as Palaeozoic to Mesozoic sedimentary rocks and these rocks are provided for the sediment deposited in the RRD. The structure of this area is confined in a straight narrow northwest-southeast aligned faulting (about 50-60 km wide and 500 km long) This major tectonic structure has used to trace southeastwards at the depth beneath the Quaternary sediment of the delta plain. The northwest-southeast alignment of the Red River fault system regulates the distribution of the sedimentary basin, the drainage area, mountainous areas, and the straight course of the Red River (Tanabe, et al., 2003). In addition, research results by Nielsen, et al. (1999) suggest that the Red River fault system has been considered minor since the late Miocene (Lieu, 2006). The Red river basin is filled with more than 3 km of Neocene and Quaternary sediments with and the subsides with 0.04-0.12 mm each year (Mathers&Zalasiewicz, 1999) (Fig 2.2).

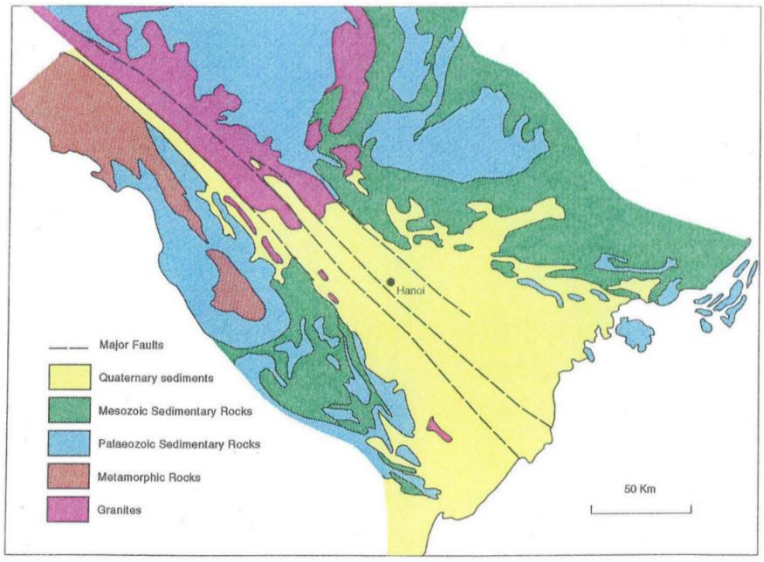

Figure 2.2. Generalized geological map of the Red River Delta and surrounds (Mathers et al. 1996)

The Quaternary sediment in the Red river basin unconformably overly the Neogene deposit, which consists mainly of sands and gravels (Pleistocene and Holocene sequences). In the RRD, the sediment is thick from a few meters in Northwest to attain about 200 m beneath part of the coastal area (Mathers&Zalasiewicz, 1999, Pruszak, et al., 2005). In the marginal parts of the delta plain, the water depths of shallow in the Gulf of Bac Bo (<50 m) indicated that the dominant Quaternary sequence is conserved on the floor (Mathers&Zalasiewicz, 1999). The Quaternary sequence within the delta plain could be classified into five geological ages: during the Holocene (Thai Binh formation, Hai Hung formation), during the Pleistocene (Vinh Phuc formation, Hanoi formation, and Le Chi formation) (Nghi, et al., 1991, Tue, et al., 2019). The simplified onshore Quaternary sequence

of the RRD researched by Vietnamese workers which consisted of two main parts: low sea-level stand sediments (along the Pleistocene) and sea level high-stand sediments (along the Holocene) (Mathers&Zalasiewicz, 1999, Tran&Nguyen, 1991).

2.2.3. Hydrology

The catchment area of the RRD is about 169,000 km^2, which originated in the mountains of Yunnan Province (China), at an altitude above 2000 m and flows 1,200 km before it drains into the sea (the Sea East, Vietnam). The annual water discharge is about 120 km^3 of water and its total sediment discharge is about 130 million tons of suspended sediment each year (ranked 15th largest in the world) (Milliman, 1995, Milliman&Syvitski, 1992). The Red River distributes its flow through five branches with 25 % of the flow of the Red River draining into the sea via the Ba Lat mouth (Pruszak, et al., 2005). The water discharge of the RRD varies seasonally, caused by most of the drainage area is affected by the subtropical monsoon season.

2.2.4. Oceanography

The Red River delta coast belong to the river-dominated coast. The coast in the north has influenced a diurnal tidal regime with a mean amplitude of 2-4 m. While the tide in the southern part is mixed with a diurnal dominance and the mean tidal range is 2-3 m (Duc, et al., 2007, Lieu, 2006). During the summer season (from April to September), tidal impacts within the delta is limited, caused by the overwhelming effect during high water drain, however, tidal impacts are evident in both major distributaries almost as far inland as Hanoi during the period from October to March of the following year (dry season) (Lieu, 2006, Mathers, et al., 1996, Mathers&Zalasiewicz, 1999).

2.3. Ao Tien Lake, Ba Be National Park (Vietnam)

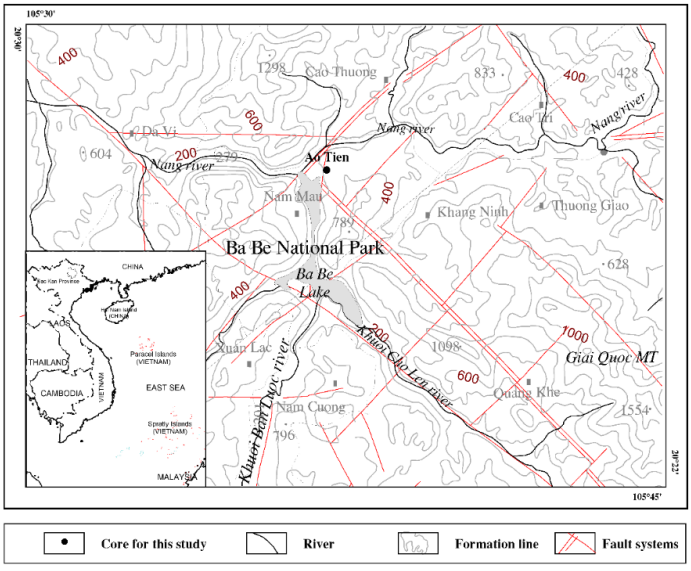

Figure 2.3. Location of Ao Tien Lake, Ba Be Lake, Vietnam

2.3.1. Geographical setting

The surrounding of Ao Tien is a limestone rock system with primaeval tropical forest. The regional climate is characterized by a tropical monsoon and it could be classified into two seasons. While in the summer monsoon from May to October with heavy rainfall, hot and humid weather. In the dry season that lasts from November to April of the following year, the climate is dry and cold (Ha, et al., 2017, Weide, 2012). The temperature of this area varied across a wide range between two seasons. The highest temperature in January and the lowest temperature in July. In the summer season, sediment from surrounding tended to increase because the increased rainfall and temperature changes lead to the raising of the deposition input at Ao Tien Lake. The source of water in Ao Tien Lake from water meteoric and groundwater exchanged with Ba Be Lake.

2.3.2. Geological setting

The surrounding Ba Be Lake is the dominant karst terrain with interspersed shale and igneous rocks. Ba Be Lake has lithology diversity (Limestone dominates the regional lithology) and tectonic unique which is resulted by long, complex geological conditions. Ba Be Lake was formed from the destruction of the South-East Asia continental mass at the end of the Cambria era (about 200 Ma) (Ha, et al., 2017), while the surrounding the ancient limestone mountains date back more than 450 million years.

2.3.3. Hydrology

Ba Be Lake is the largest natural freshwater lake in Vietnam with four rives and streams which connected to the lakes. Cho Leng River, Ta Han and Bo Lu streams, all in the south and southwest which pour water in the lake with the total catchment area of 420 km^2. Lake outflow water in the Nang River through several waterfalls and subterranean caves and then continues to flow in the Gam River.

2.3.4. Biodiversity

Ba Be National Park is rich in biodiversity and owns typically ecological features of lowland evergreen forests, lakes on mountains, and evergreen forests on limestone mountains. Ba Be National Park is home of 1,281 plant species, which includes 25 species that are listed in the Red Book of International Union for Conservation of Nature (IUCN). Moreover, many rare plants are listed in The Vietnam Red Book as well. Not only having a diverse flora, but Ba Be National Park also owns a rich fauna in terms of both quality and variety. Scientists found here 81 mammals, 27 reptiles, 17 amphibians, 322 species of birds, 106 fish species, and 553 species of insects and mites. Up to now, there are 66 rare and endemic species listed in the Red Book of both Vietnam and the world.

CHAPTER 3. METHODOLOGY

To create an overview of the methods used in thesis, a flowchart illustrates the methods and in which order they are completed (Fig 3.1)

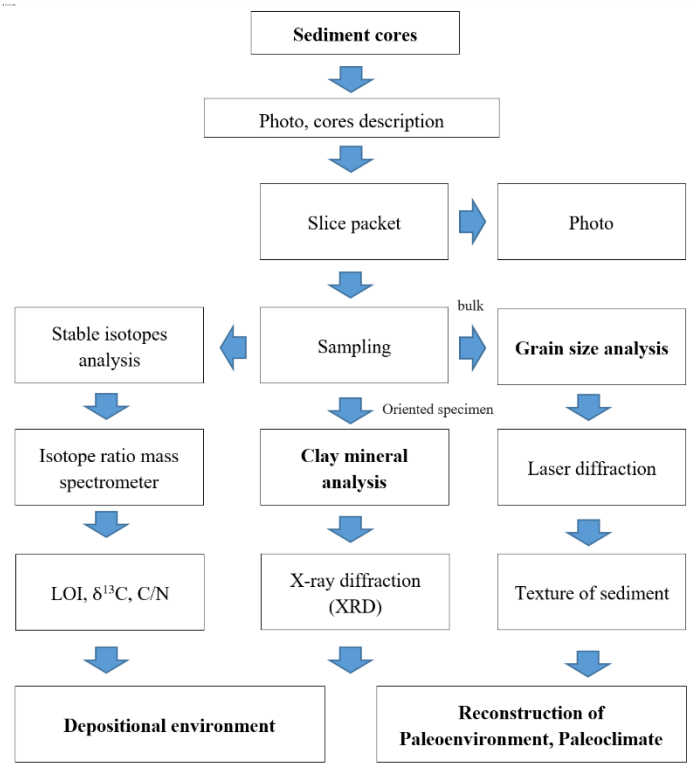

Figure 3.1. Flowchart illustrating the research process

3.2. Taking sediment core samples

A core sample of the RRD was collected by rotary drilling techniques which was based on a few principles: to avoid disturbances to sediments; to preserve the status quo of drill cores; enhanced core recovery. The sediment core was immediately separated into pieces of 1 m in length. During the drilling processes, disturbing sediment surfaces (about 20 cm) were rejected. Sandy materials were often gone lost because no core catcher was mounted on the coring tube. Therefore, it was described as detail in describing as drill cores. From this information, this study was collected drilling cores taken from the RRD with the geographical location at latitude 20°25'39.86" N, longitude 106°24'7.46" E, altitude +0.5 m. The depth of sediment core in RRD is about 36 m and core recovery was 80 %. Directly following a collection, the core sample was described preliminary, settled in PVC tubes and sealed in aluminium foil. Then it was delivered to the laboratory in cool condition. In the laboratory, core samples were processed during 12 h of collection by first removing the outer layer (~0.5 cm in thickness), then the cores were sliced in 20 cm portions.

Sediment core (AT) was collected by a rotary drill. The core sample located at latitude 22°26'51.35" N, longitude 105°37'2.64" E, in 14 m deep water. The total core length was 108 cm and sediment recovery approached 100 %. Directly following a collection, the core sample was decribed the preliminary, settled in PVC tubes and sealed in aluminium foil. Then, it was preserved in cool condition and delivered to the laboratory. In the laboratory, sediment cores were divided and tested on thee basis of grain-size, sediment textural, color and crushed shells. The outer layer (1 cm in thickness) was removed which minimized contamination, then the cores were sliced in 2 cm portions (54 samples).

3.3. Grain size analysis

In the laboratory, all samples were first dried in an electric oven at 60 °C (during 48 h). The dried sample put in a mortar and slightly crushed by a rubber pestle. Organic matter, carbonate, and silica were removed using 30% H_2O_2, 20% Ac and 2 mol/l sodium carbonate, respectively. For the sediment grain size it was used laser beam diffraction, using a Particular LA-950 (Horiba) instrument at the GEO - CRE (Key Laboratory of Geoenvironment and Climate Change Response), Vietnam National University (VNU) (Fig 3.2). This device can measure suspension samples liquid in the grain size range of 0.05 - 3000 μm. The sediment grain size was analyzed in triplicate for each sample with a relative error of at most 1 %. The sedimentary parameters were determined based upon the distribution of grain size and statistics software (GRADISTAT program) (Blott&Pye, 2001).

The grain size parameters include: mean grain size (Mz), sorting coefficient (So), skewness (Sk), kurtosis (K_G).

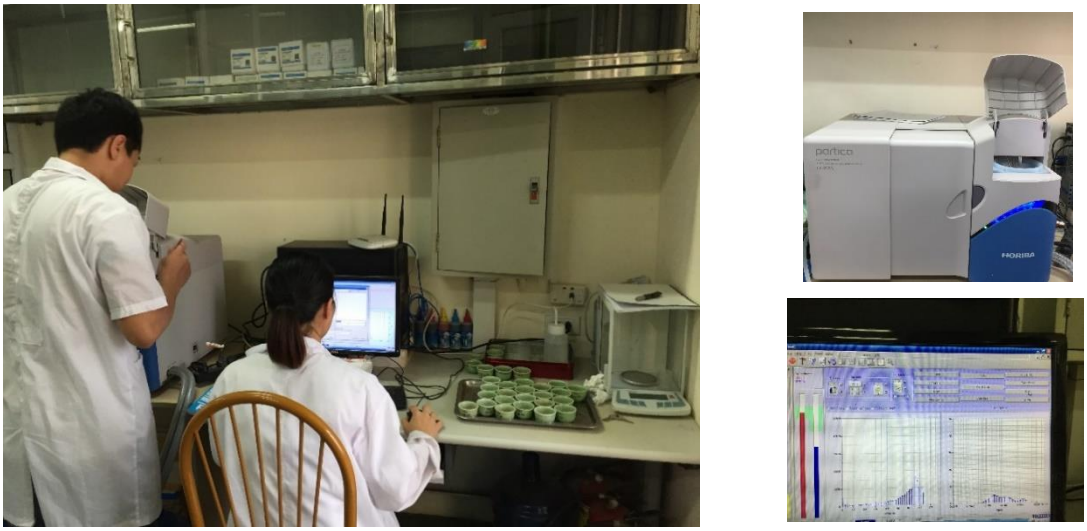

Figure 3.2. Preparation and measurement of the grain size analyses were completed at the Key Lab (Vietnam National University - VNU)

3.4. X - ray diffraction analyses (XRD)

X-ray diffraction analyses were completed at the University of Bucharest, Romania. For the determination of clay minerals by X-ray diffraction was required to complex sample preparation to increase the intensity of diffraction reflexes. Wet sediment sample (25 g) were split and disaggregated with distilled water because dry grinding can cause changes in the phase, and in extreme cause, can lead to stress defects in the structure of crystals which will show XRD line diffracted or even structural collapses (the production of X-ray amorphous material) (Moore&Reynolds Jr, 1997).

All samples were treated to remove organic matter, carbonate and silica with 10 % H_2O_2, 20 % H_2COO_3 and 2 mol/l sodium carbonate (Kunze&Dixon, 1986, Rabenhorst, et al., 1984). At the moment the effervescence ceased, the excess acid is removed by repeated washings with distilled water and centrifugations. Particle grains were separated by settling due to Stoker's law and concentrated by centrifugations.

After treatment with sodium polyphosphate, the samples were centrifuged several times for fraction separation < 2µ. The separation of dispersed suspension in 2 rotating test tubes with 5 ml. The first tube was saturated by $MgCl_2$ and the second tube was saturated by KCl and each tube was transferred to two slides by wet smearing. The smear samples were performed also on oriented specimens with combined of air-dried condition, glycerol solvation, heated at 330 °C and 550 °C (Jackson, 2005).

The analysis was performed semi - quantitatively using a PANalytical diffractometer in the following conditions: Oriented sample was saturated by $MgCl_2$ and air-dried at 20 °C; Oriented sample was saturated by $MgCl_2$ and solvations with ethylene glycol and glycerol, heated to 80 °C during 8 -10 hours (vapour method); Oriented sample was saturated by KCl and air-dried at 20 °C; Oriented sample was saturated by KCl and heated to 330 °C during 1 hour; Oriented sample was saturated by KCl and heated to 550 °C during 1 hour.

The heated, solvated, saturated and the air-dried sample was kept in a desiccator until they were analyzed. X-rays are electromagnetic radiation same to light (with a great shorter wavelength). The wavelength of X-ray and the structural spacing's of crystals both have dimensions about angstroms (1Å = 10^{-8} cm). X-rays are produced when electrons that have been accelerated to high speeds collide with a target metal (Poppe, et al., 2001). In X-ray tube, these electrodes were maintained under a high voltage and lead to the electrons toward a metal target (the anode). (Moore&Reynolds Jr, 1997, Poppe, et al., 2001).

When an incident X-ray beam encounters a crystal lattice, normally, occurrence scattering. In spite of almost interferes by itself and it also was eliminated (destructive interference), diffraction occurred while scattering in a direction certain, which was in the same phase together scattered rays from other atomic planes. In this condition, the scattered X-ray got together to form new increased wavefronts respectively reinforce each other (constructive interference) and they are formed at the point of influence, and radiate in all directions. The connection by which diffraction scattering appearances is known as the Bragg law or Bragg equation. Each crystalline material was diffracting X-rays in a unique characteristic pattern, caused by it had a characteristic atomic structure.

This Bragg's law is expressed in a mathematical form a equation:

$$n\lambda = 2d \sin\theta$$

where: d - the distance (nm) between the lattice planes; θ - the Bragg angle; λ - a wavelength of the characteristic X-ray; n - the order of reflection.

Based on the model of Bragg, the layers of the clay minerals can be regarded as network levels. Oriented specimen preparation has been used for the determination of the clay minerals. The analysis was run with X-ray Diffractometer (PANalytical X'Pert Pro) at the Mineralogy Department, University of Bucharest, Romania. The PANalytical X'Per Pro diffractometer has two main parts: the Co X-ray tube and the very fast X'Celerator detector. Diffraction data was achieved by exposing powder samples to Cu-Kα X-ray radiation and it has a characteristic wavelength (λ) of about 1.54 Å. X-rays were created from a Cu anode due to provided with 40 kV and a current of 40 mA. The data was recorded with a scan speed of 1.0 ^{o} min^{-1} and a step size of 0.01 ^{o} in the 2θ range of 4-40 degrees. During operation of the machine, the stability and accuracy of the mass spectrometry systems need to test before driving.

Mineral identification

Diffractograms were visually interpreted with the help of a computerized search via PANalytical X'Pert HighScore Plus, v3.0 program. The peak area values of clay minerals used to calculate percentages of major clay minerals. Clay minerals reflect X-ray beams in the various direction because they are formed of numerous crystal lattices arranged in a certain manner. If a mineral has a high amount in the smear sample, after analysis, its peak will appear with high intensity and high value of peak area. Based on the semi-quantitative method, clay minerals in RRD sediment are determined (Biscaye, 1965, Starkey, et al., 1984). Besides, the diffraction peaks could be occurred for all the other d (00l) reflections within the two theta interval scanned where there is no mixed layer.

Illite is one of the mica clay mineral series and it is structurally similar to muscovite. Illite is identified by a series of X-ray diffraction peaks at 10 Å (00l) and 3.3 Å (003) peaks which are not

appreciably affected by heat treatment (to 550 °C), glycerol or ethylene glycol solvation and K-saturated (Fanning, et al., 1989, Poppe, et al., 2001). In many cases, the value of the area in peak 10 Å (from the air-dried sample) was suggested for the calculation of illite percentage. The degree of crystallization of illite was determined by illite well-ordered (10.0 Å) and illite poor ordered (10.2 Å) (Meunier, 2005) (Table 3.3).

Kaolinite and chlorite were separated into the relative intensities of their 3.58 Å (002) and 3.54Å (004) peak, respectively (Biscaye, 1965). Besides, heating alone will not determine the dioctahedral kaolinite group minerals from chlorite (iron-rich), caused by the 002, 003, and 004 chlorite peaks are also weakened during this heat treatment (Moore&Reynolds Jr, 1997). The area of peaks in air-dried smear samples represent the behaviour of kaolinite, chlorite, respectively. Kaolinite and chlorite can be differentiated by heating because Chlorite (about 14 Å) is typical heat stability. When the sample is heated at 550 °C to destroy the kaolinite and may weaken or destroy the chlorite (7 Å), the chlorite structure is left largely intact with only partial dehydration of the octahedral layer (Brindley&Gillery, 1956) (Table 3.3).

Smectite is characterized by basal reflections (yield X-ray diffraction patterns typical). When heated to 500 °C, the 001 reflection will collapse to about 10 Å (the exchange cations) (Moore&Reynolds Jr, 1997). When Mg-saturated, the 00l reflection will swell to about 17 Å (approximately 17.8 angstroms with glycerol). The value of area of peak 17 Å has been used to identify this clay mineral in several cases (Table 3.3).

3.5. The grain density analysis

This method was accomplished to determine the mass of sediment per unit of volume which is calculated by:

$$\rho = \frac{(M3 - M1)}{V}$$

The grain density was analyzed and performed according to the following steps: the plastic container was marked and then it was weighted using calculations (M1). The amount of sediment was taken into the plastic container (with the unit volume - V is 1 cm^3). After that, the weighing before (M_2) and after (M_3) drying in oven (at 60 °C during 48 h) until the amount is constant.

3.6. Organic matter analysis

The organic matter (OM) content was determined via loss on ignition measurement (LOI). About ten grams of fresh sediment was put into a beaker and completely dried at 60 °C (in the oven) and then ground to a fine powder by using an agate mill. During grinding, extraneous materials as small plant matter and shell fragments, which were manually eliminated using forceps (by stainless

steel). About 2 grams of the pulverized sediments were first dried at 100 °C in a drying oven (during 2h) and then heating at 550 °C in a temperature monitored muffle furnace (during 3 h). Organic matter content is calculated based on the inequality between the weight from before and after heat treatment processed (at 550 °C), which divided by the initial sample weight times 100 % (Tue, et al., 2014).

3.7. Stable isotopes analysis

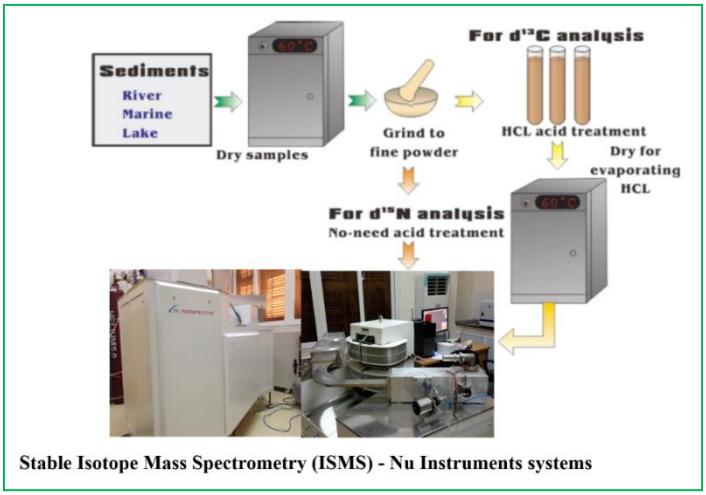

Figure 3.3. The processes of pretreatment and the treating sample for Stable isotopes analysis (Using Stable Isotope Mass Spectrometry (ISMS) - Nu Instruments systems)

For analysis of stable carbon isotopes ($\delta^{13}C$), and C/N ratios, the fresh sediment was put into a beaker and completely dried at 60 °C (during 48 h), and then grounding to a fine powder by using an agate mill. The extraneous materials (as small plant matter and shell fragments) were removed using forceps (by stainless steel). After that, 0.2 g of pulverized sediment was put in an Eppendorf tube and treated with HCl 1N for 24h to remove carbonate at room temperature. Then, the samples were rinsed by 4 ml Milli-Q filtered with distilled water. This process was repeated four times before being dried in an oven at 60 °C (during 48 h), following the methods outlined by Tue *et al.*, (2014). After dried, about 10 g samples were weighed and wrapped in tin capsules. The $\delta^{13}C$, C/N ratios were measured using a stable an isotope ratio mass spectrometer (Nu-Perspective Instrument) system at the GEO - CRE (Key Laboratory of Geo-environment and Climate Change Response), Vietnam (Fig 3.3). After the analysis, a certified reference material (L-alanine) has been used to quantify the analyzed results. The $\delta^{13}C$ was expressed in ‰ (per mil) and the following equation:

$$\delta X(‰) = \left(\frac{R_{Sample}}{R_{Standard}} - 1\right) * 1000$$

Where, δX is $\delta^{13}C$ or $\delta^{15}N$; R = $^{13}C/^{12}C$ or $^{15}N/^{14}N$, R_{sample} is the isotope ratio of the sample and $R_{standard}$ is the isotope ratio of a standard reference to Pee Dee Belemnite (PDB) limestone carbonate.

CHAPTER 4. THE LITHOLOGY, GEOCHEMICAL PROXIES, CLAY MINERAL CONTENT OF SEDIMENT

4.1. Red River Delta

4.1.1. Lithological characteristics

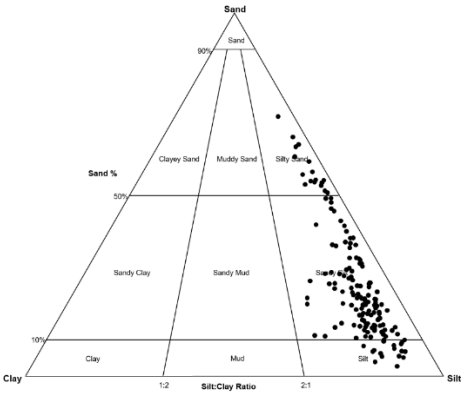

Figure 4.1. Tri-plot for textural analysis of all sediments in core sample RRD

The sediments of core samples are comprised mainly of clay, silt, and sand, which varied from 1.5-25.5, 22.9-87.2, and 3.3-73.4%, respectively. According to textural analysis in the core sample, sediment facies could be classified as sandy silt, silty sand, and silt (Fig 4.1). While based on lithology characteristics, color, and texture parameters, the sediment could be classified into six sections and two-second sedimentary units: unit 1- estuarine sediments; unit 2 - deltaic sediments. The depositional condition of the RRD has resulted in the interaction between sea-level changes and fluvial inputs along the Holocene.

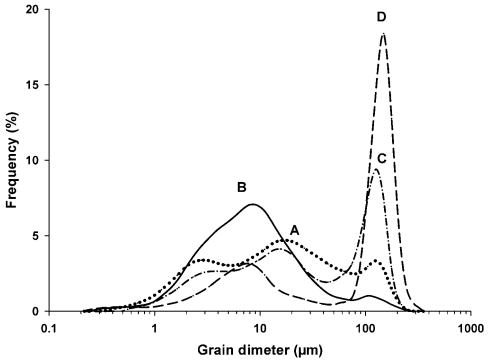

Figure 4.2. Grain-size distribution in the sediment core of the RRD: (A), (B), (C) and D sediments

According to the character (lithology) of sediment core, it showed a correlation with the core VN from the last studies in RRD (Li, et al., 2006, Tanabe, et al., 2006). Consequently, the sediment geochronology of this study was estimated according to the sediment rates, which was identified based on accelerator mass spectrometry radiocarbon dates (AMS-^{14}C). The result showed that the last core length corresponds to dates ranging from 11.26 cal. kyr BP (Tue, et al., 2019).

a) Mz and So **b) Sk and So**

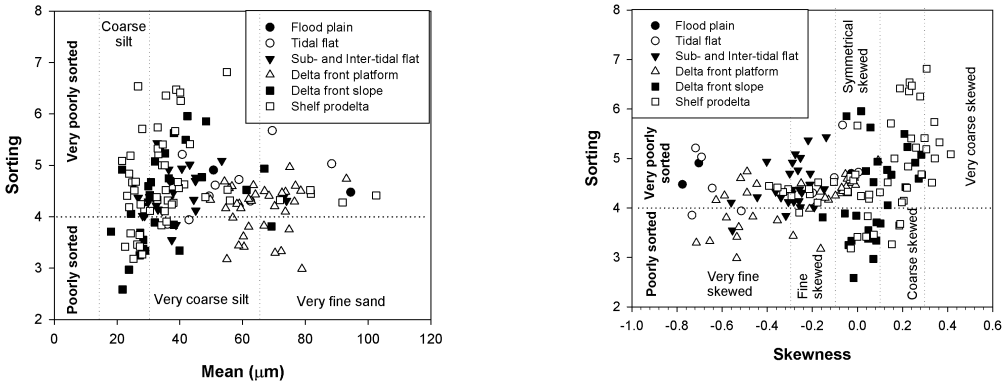

c) Sk and KG

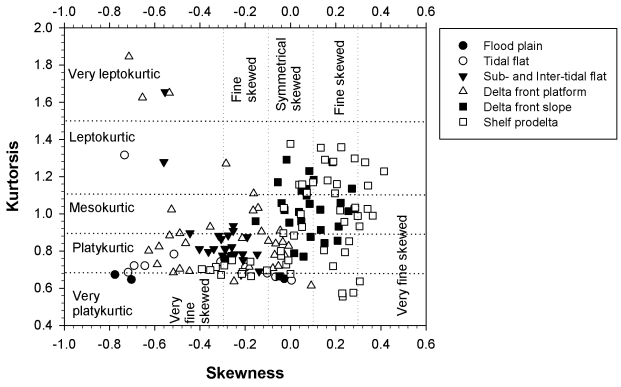

Figure 4.3. The bivariate relationship between: (a) the mean grain-size (μm) and sorting, (b) skewness and sorting, (c) skewness and kurtorsis

Based upon the grain-size analyses, the sediment core revealed the fourth types of grain-size categorization: For type B, a large portion of the samples (46 %), displayed a bimodal grain-size categorization with a modal size of 10-40 μm and a small number of fine material. Type A and C, which just occupied 31 % and 19 % of the total samples, respectively and displayed a trimodal grain-size categorization. Type D showed bimodal grain-size categorization, with similar modal size of the fine grain-size and a different modal size of the coarse grain size (Fig 4.2).

According to the assumption of these statistical parameters, reliability reflects differences between different deposition settings. Figure 4.3a illustrates the correlative between mean grain-size (Mz) and sorting (So). For third deposition environments (sub- and intertidal flat, tidal flat, floodplain), there is clustering in fine-sized and very poorly sorted. Both Mz and So are hydraulically controlled (Rajganapathi, et al., 2013) so that in all sedimentary environment the poorly sorted sediments have a mean grain-size in the medium silt fraction. Figure 4.3b illustrates the correlation between skewness (Sk) and sorting. For the sub-to intertidal flat and delta front flatform, sediment is

displayed very poorly sorted and symmetrical to very fine skewed. By contrast, poorly sorted to very poorly sorted are chiefly clustered around symmetrical to fine skewed and negative skewness values. For the delta front slope and shelf prodelta sediment, poorly sorted to very poorly sorted are mainly clustered around very coarse to symmetrical skewed and have positive skewness value. In figure 4.3c illustrates the correlation between skewness and kurtosis (KG). For the delta front slope and shelf prodelta sediment, the positive skewness/very platykurtic to the very leptokurtic. Others deposition environments, the negative skewness/very platykurtic to the very leptokurtic. This pattern showed the mainly of a silt grain-size population and the subordinate of very fine sand grain-size which gives a small proportion of negative skewness.

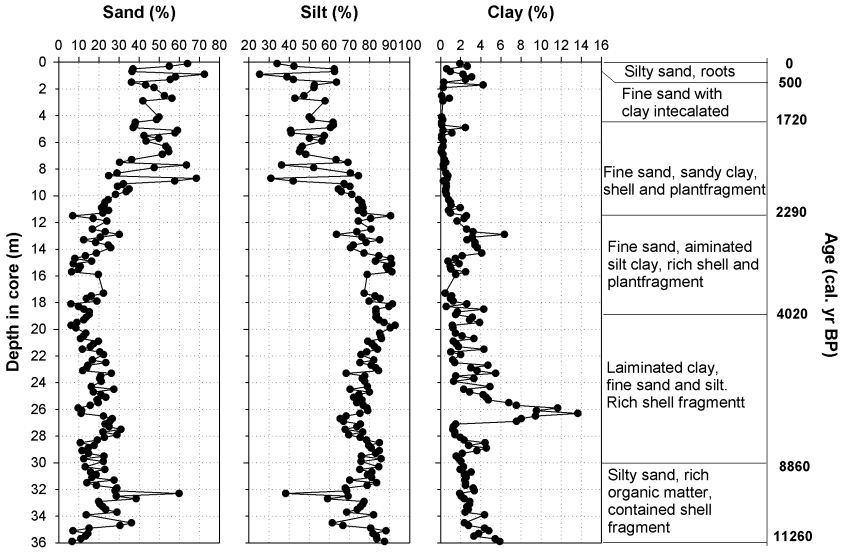

Figure 4.4. Grain-size distribution of the sediment core in RRD, Vietnam

a. Core section 1: at the depth from 36 to 30.1 m

In this section, sediment is characterized by reddish-gray and consisted of very fine sand with clay lamination (as faint lenses 3-8 mm thick) and a large portion of this facies is bioturbated. Mud content of the sediment slightly decreases from the depth of 36 m to the smallest value (at the depth of 32.3 m) (Fig 4.6). The Mz tended to slightly increase upward with average value was 18.39 µm. The average value of So was 4.45±0.4 and a large portion of the value is classified as very poorly sorted. The mean of Sk ranged -0.29±0.1, it is categorized as very fine skewness and fine skewness sediment. KG values tended to increase upward with two high values were 1.65, 1.28 at the depth 32.3 m, 31.3 m, respectively. The KG value could be classified into three types, but a large portion value indicated platykurtic sediment (Fig 4.5).

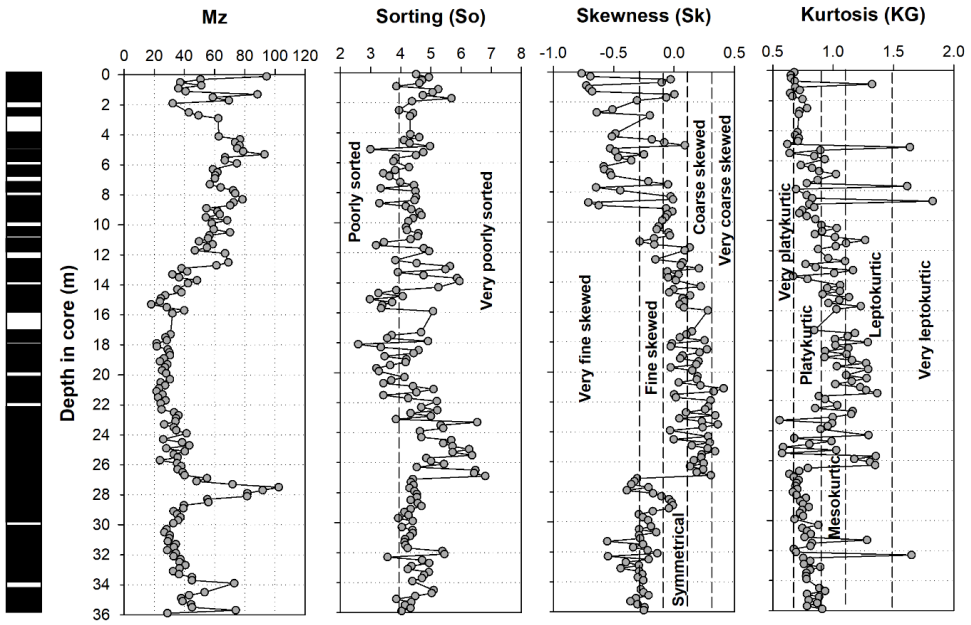

Figure 4.5. Depth variation of sedimentary parameters (Mz,So, Sk, KG) in the core sample of the Red River Delta

b. Core section 2: at the depth from 30.1 to 18.9 m

In the section, surface erosion formed during a transgression and separated by others section (depth core sample about 30 m) (Tanabe, et al., 2006). The feature's sediment is blue-gray and composing of laminated silt, fine sand with reddish-gray in color. Besides, sediment was bioturbated by gray clay and rich in shell fragments. Mud values in this section ranged from 69.16 to 95.48 %. Most notably, Mz values tended to slightly increase upward from the depth of 30.1 m (the erosion surface) to the depth of 27.5 m and decreased to the depth of 18.1 m. The value of So were classified into two types with a high portion of values was very poor sorted sediments (30-21.9 m of the depth sediment core) and others were poorly sorted sediments. Based on Sk values, sediments could be classified into 4 types, including coarse skewed, symmetrical, fine skewness and very fine skewness sediments. According to KG values, indicating that platykurtic sediments (at the depth core between 30.1 and 26.5 m) and the upper layer has shifted in a high range which indicated form very platykurtic to leptokurtic.

In the middle of the Holocene, the sediments comprised of two parts. At the lowest part, sediment facies could be a ravinement surface, which based on the transport sediment process (Li, et al., 2006, Tanabe, et al., 2006). At the depth from 30.1 to 27.5 m, sediment core showed the transgressive sand layer overlie the erosion surface, characteristics of Sk corresponds to lower energy condition, suggesting the abundant origins of sediment inputs. Between 26.7 and 18.7 m in depth of core sediment, the Mz and Sk values varied over a small range, which corresponds to low

hydrodynamic energy conditions. The dominance of mesokurtic and leptokurtic sediments suggested the coarse grain-size was continuous added.

c. Core section 3: at the depth from 18.9 to 11.7 m

In this section, sediment consisted of reddish-gray and black with laminated silt clay. Mz values between 6.40 and 20.49 µm and tended to gradually increase upward. Mud content tended to slightly decrease with ranged from 70.77 to 96.70 %. Sk values were gradually decreased upward and classifying it as symmetrical and coarse skewed sediment. The values of kurtosis showed relative low variation from 0.69 - 1.29, classified as platykurtic, mesokurtic and leptokurtic sediment. In this section, Mz values and sand content slightly increased upward which indicated higher hydrodynamic energy.

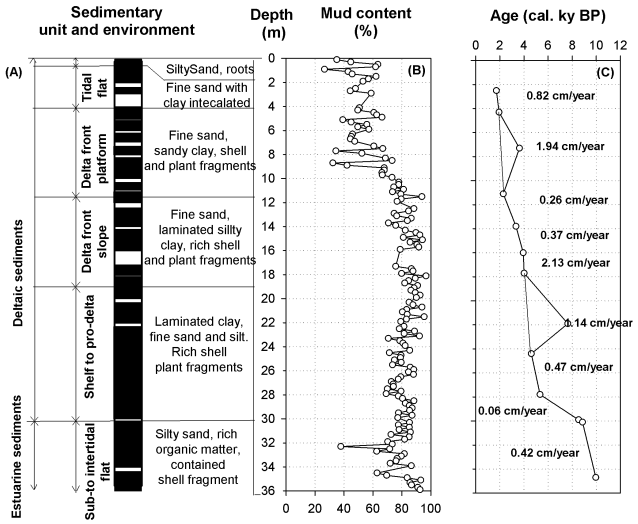

Figure 4.6. Sedimentary columns of the core sample in RRD. (A) Lithological characteristic of sediment core; (B) Mud content in sediment core; (C) Sedimentation rates were determined by linear interpolation between radiocarbon datings (^{14}C) (Li, et al., 2006)

d. Core section 4: at the depth from 11.7 to 4.1 m

Sediment has consisted of gray clay and fine sand with rich plant matter. Mud values in sediment tended to decrease and the minimum value at the depth of 8.7 m (32.4 %). Mz values tended to increase and ranged between 11.06 and 56.55 µm. So values were a small range from 2.99 to 4.97 with mainly categorized very sorted sediment. Sk value fluctuated and indicated as symmetrical, fine skewed and very fine skewed sediment. KG values fluctuated and predominantly indicating platykurtic and mesokurtic sediment.

The rate of sediment markedly up to 1.94 cm per year in this section during the increasing of delta progradation (Hori, et al., 2004, Li, et al., 2006, Tanabe, et al., 2006), indicating the sediment supplied to the river over the last 2 cal. kyr BP was different than the volume of sediment redistributed

or rework which affected by longshore current and waves (Li, et al., 2006, Tanabe, et al., 2006). The coarsening succession upward which suggested that the energy of the environment increased.

e. Core section 5: at the depth from 4.1 to 0.5 m

In this section, sediment is featured by silt, fine sand, silt with gray in color and minor peat lenses 1-5 cm thick. Sand content tended to slightly increase upward with a maximum value (36.5 %) at the depth of 0.5 m, whilst, Mud content tended to decrease. Mz values changed in a wide range at the depth from 4.1 to 1.7 m and then suddenly rose to values of 88.38 μm (at 1.7 m in depth). The upward increasing trends of So values and reached the maximal value (at the depth of 1.7 m). In this section, the sediment is dominated by very poorly sorted. While Sk values continuously fluctuated and classified from very fine skewed to fine skewed sediments. The values of KG varied over a small range with the exception of the depth interval from 0.8 to 1 m. The dominance of sediment is classified as platykurtic sediments. The increasing of clay content and a decrease in the values of Mz suggested the decline of wave energy and tidal.

f. Core section 6: at the depth from 0.5 to the core surface

Sediments in this section consisted of reddish-brown mottled clay with abundant rootlets because it corresponds to a lateritic weathering profile develop in the floodplain (Tanabe, et al., 2006). The upward increasing trends of mean grain-size. According to the values of sorting, sediment could be classified as very poorly sorted. While, the values of the kurtosis ranging between 0.64 and 0.67, suggesting that the size distribution was platykurtic sediment. Sand content was from 36.5 to 64.9 % and mud content fell to the lowest percentage (35.08 %) which suggested the sediments formed in a high energy environment. The Mz values in the surface were high because it was influenced by channel-levee sediment at the land surface of the core-site.

4.1.2. Geochemical proxies (LOI, TOC, $\delta^{13}C$)

In the depth sediment core from 36 to 30.1 m, LOI values fluctuated with an average of about 4.4 %. The upward decreasing trends of LOI values at the depth from 30.1 to 26.7 m and then increased to the maximal values of 21.3 m in depth. LOI values continuously decreased in the depth sediment core between 21.3 and 4.1 m, then slightly increased again from 4.1 to surface sediment core.

C/N ratios shifted from 3.53 to 20.08 with an average of 11.09 ± 3.4 (Fig 4.7). Most notably, the ratios fell sharply to 6.7 at the 30.3 m in depth (the erosion surface). In the depth from 36 to 30.1, C/N rations fluctuated slightly, then it tended to increase upward from 30.1 to 17.3 m in depth. At the

depth from 17.3 to 7.7 m, C/N ratios tended to decrease to the lowest value (3.5) at 7.7 m in depth and then fluctuated to the core surface.

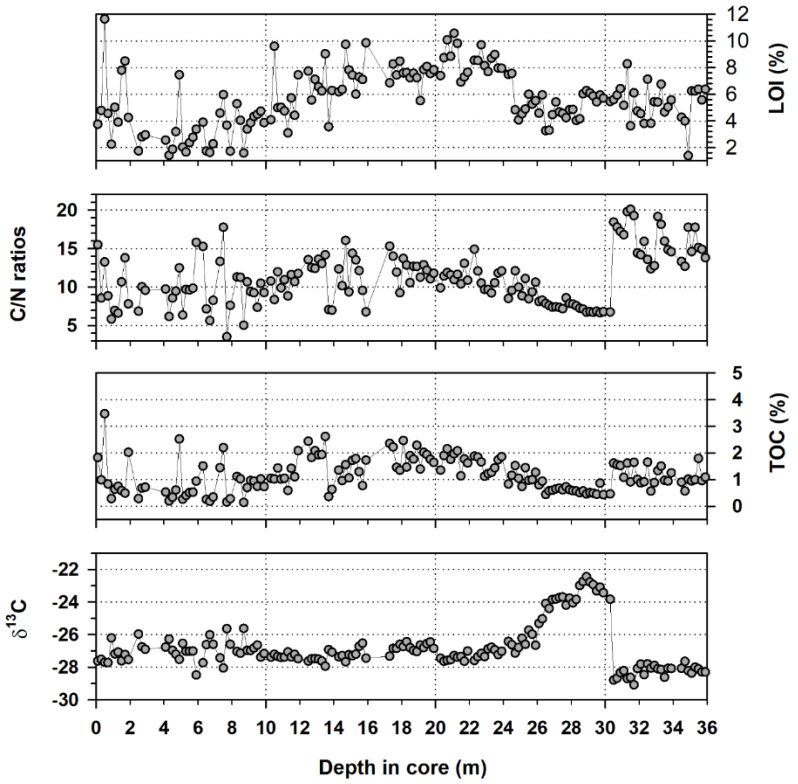

Figure 4.7. The variation of LOI (%), C/N ratios, TOC (%) and $\delta^{13}C$ (‰) in sediment, Red River Delta with depth (m)

Below the depth of 30.1 m, TOC content gradually fluctuated with an average of 1.1±0.4 % and notice a suddenly decreased (0.45) at the depth of 30.3 m. TOC content varied over a small range at the depth sediment core from 30.3 to 26.5 m, then it tended to decrease between 17.3 and 4.1 m with three exceptions (at the depth of 4.9, 7.5, and 14.7 m). TOC values tended to increase at the depth from 4.1 to surface sediment core.

The linear regression of TOC content and LOI content indicated that the LOI method could be used to assess TOC content in the sediment. Also, there was a strongly significant positive correlation between TOC and total nitrogen (TN). The regression line for these data approached very close to the origin, which suggested the inorganic nitrogen content was insignificant and the total nitrogen was chiefly in organic nitrogen. Consequently, the total nitro could be used to calculate C/N ratios, which determined the origins of sediment and reconstruction of the Holocene paleoenvironment (Lamb, et al., 2006, Müller&Mathesius, 1999).

$\delta^{13}C$ values varied from -29.09 to -21.95 ‰ with an average of −26.79±1.4 ‰. Most notably, it suddenly increases to a value of -23.84 ‰ (at 30.3 m in depth). $\delta^{13}C$ values had small fluctuations

from 27.02 to 29.09 ‰ at the from 36 to 30.5 m, then rose and reached the highest value (-21.9 ‰) at the depth of 28.9 m. Between 29.8 and 20.3 m in depth, $\delta^{13}C$ values tended to decrease. At the depth between 20.3 and 8.7 m, $\delta^{13}C$ value was relatively invariant, then fluctuated to the core surface sediment. Generally, $\delta^{13}C$ values displayed an opposite trend with C/N ratios.

4.1.3. Clay mineral content

Illite contents ranged from 13.29 to 78 % with an average of 60.46±17.45 %. Below the depth of 28.1 m, illite contents fluctuated extensively around the mean 49.78±15.90 %. Illite contents tended to increase from 28.1 to 24.3 m in depth, then slightly fluctuated between 24.3 and 2.9 m with a mean of 59.37±12 %. From 2.9 m to the core surface, illite contents tended to increased (Fig 4.8).

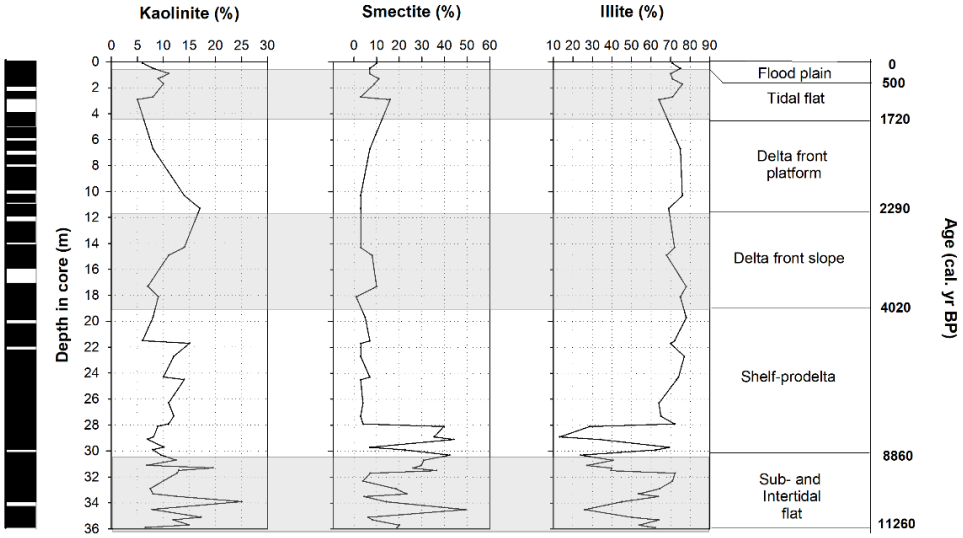

Figure 4.8. Variation in clay mineral (smectite, kaolinite and illite) proportion (%) in the core sediment of RRD, Vietnam

Kaolinite contents ranged from 5 to 25 % with an average of 10.75±3.95 %. Below the depth of 30.1 m, kaolinite contents fluctuated around the mean 12.19±5.05 % and reach a peak to a maximum at 33.9 m. In the section between 30.1 and 21.6, kaolinite contents tended to increased and then suddenly fell at the depth of 21.8 m. Kaolinite contents continuous increased at the depth between 21.6 and 11.3 m, then slightly decreased of 2.9 m in depth. From 2.9 to 0.9 m in depth, kaolinite tended to increase and then drop at the depth from 0.9 to the core surface (Fig 4.8).

Smectite contents ranged from 1 to 49.33 % with an average of 14.24±13.34 %. Below the depth of 28.1 m, smectite contents fluctuated widely from 4 to 49.3 %, then suddenly dropped at the depth of 27.9 m , smectite contents fluctuated again at the depth from 27.9 to 14.2 m, then increase upward at the depth of 2.9 m. Smectite tended to fluctuate at the depth from 2.9 m to the core surface. In comparison, variations in the two most abundant ones (smectite and illite) have opposite trends.

4.2. Babe Lake

4.2.1. Lithological characteristics

. The dominance of sediment composed of sand, silt and ranged from 6.04-27.67 %, 72.33-93.96 %, respectively. The clay fraction content displayed very small. The color of sediment is characterized by dark gray bands, it suggested that sediments could be formed in an aerobic environment because the depositional environment occurred in the lake bottom.

a. Core section 1: from 108 to 90 cm

In this section, sediment is characterized by sandy silt and composed of the fine sand and coarse silt. Mud content varied in cross a wide range from 76.01 to 83.58 %. The mean sediment grain size fluctuated slightly between 23.73 and 33.63 µm with a mean of 29.12±3.21 µm. In this section, the mean sorting (So) value ranged from 2.96 to 3.42, classifying it as being very poorly sorted sediment. The skewness (Sk) values were ranged between 0.3 and 0.36 with a dominance of very coarse skewness sediment.

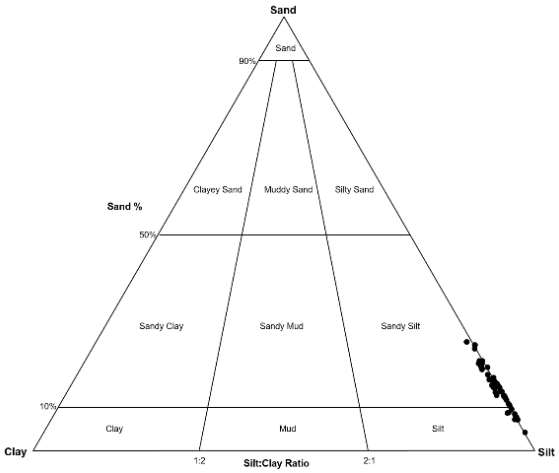

Figure 4.9. Triangle graph of grain-size composition

b. Core section from 90 to 23 cm

This section consisted of coarse silt, medium silt, and fine sandy. The increasing trends of mud content and reached the highest value (93.96 %) at the depth of 51 cm. Mz values fluctuated widely and reached the maximum (28.97 µm) at the depth of 81 cm. So values were closely correlated with the Mz values. According to the different of So values, the dominance of sediment could be classified as poorly sorted. Sk values fluctuated widely, suggesting is as very coarse skewness to coarse skewness sediments (Fig 4.10).

c. Core section from 23 to 0 cm

In this section, sediment is characterized by fine sandy and medium silt. Mud content markedly decreased upward to the depth of 13 cm (72.33 %), before continuously increasing to the

sediment core surface. Mean grain size tended to rise to the value of 30.75 µm at 13 cm in depth, before decreasing upward. So values were also closely correlated with the Mz values. In this section, sediment categorized the dominant poorly sorted. Sk values can be separated into two-part. In the first part (from 23 to 9 cm), the Sk values tended to increase to value of 0.48, however, the Sk values from 9 cm to surface sediment core tended to decrease and the dominance of sediment is classified as very coarse skewness (Fig 4.10).

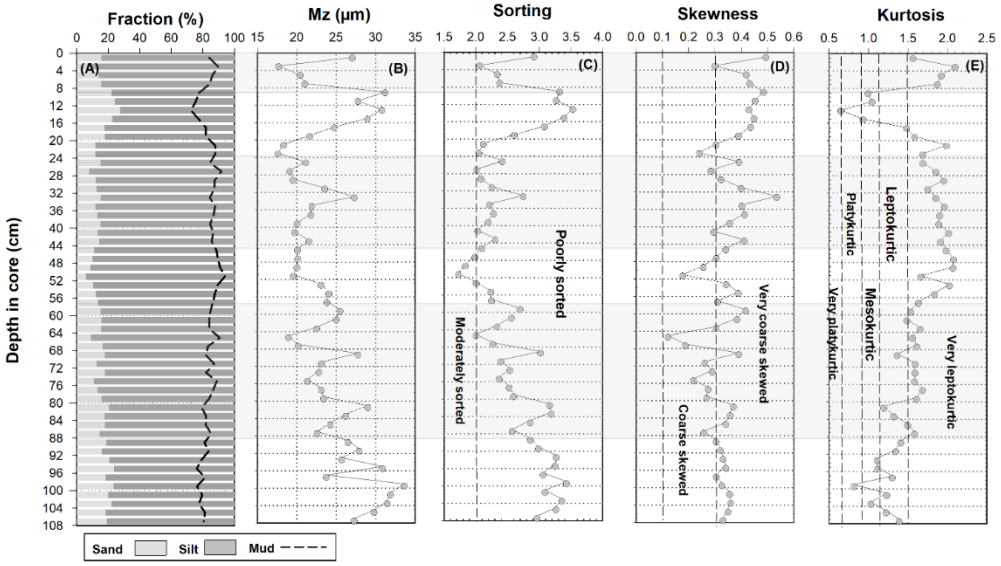

Figure 4.10. Depth variation of sedimentary parameters (Mz,So, Sk, KG) and grain size distribution in the core sample AT

4.2.2. Geochemical proxies (OM, C/N ratio, $\delta^{13}C$)

Organic matter is estimated from performing the loss on ignition (LOI). LOI values varied across a wide range from 5.19-20.69 %, with an average of 12.69±4.88 %. Below the depth of 91 cm, LOI values tended to slightly increase with a maximum at the depth of 95 cm (20.69 %), then dropped at the depth of 53 cm. LOI values content fluctuated with a small range at the depth from 53 to 27 cm, although LOI values displayed a two peak at depth of 41cm, 31 cm with ranged 10 %, 10.45 %, respectively. At the depth between 27 and 15 cm, LOI values tended to increase, then continuously decreased upward (Fig 4.11).

Organic carbon content ranged from 16.67-36.55 % with an average of 26.2±6.44 %. At the depth below 57 cm, OC content varied over a small range and tended to slightly increase. From 57 to 27 cm, OC content displayed higher variation and then decreased to the surface sediment (Fig 4.11).

C/N ratios varied in values from 10.68 to 17.01, with an average of 13.23±1.3. Below 91 cm, ratios tended to gradually increase upward, then slightly decreased at the depth of 23 cm. Between

23 and 9 cm, the upward increasing trends of C/N ratios and then relatively stabled from 8 m to the core surface. Generally, C/N ratios were quite closely correlated with the LOI values (Fig 4.11).

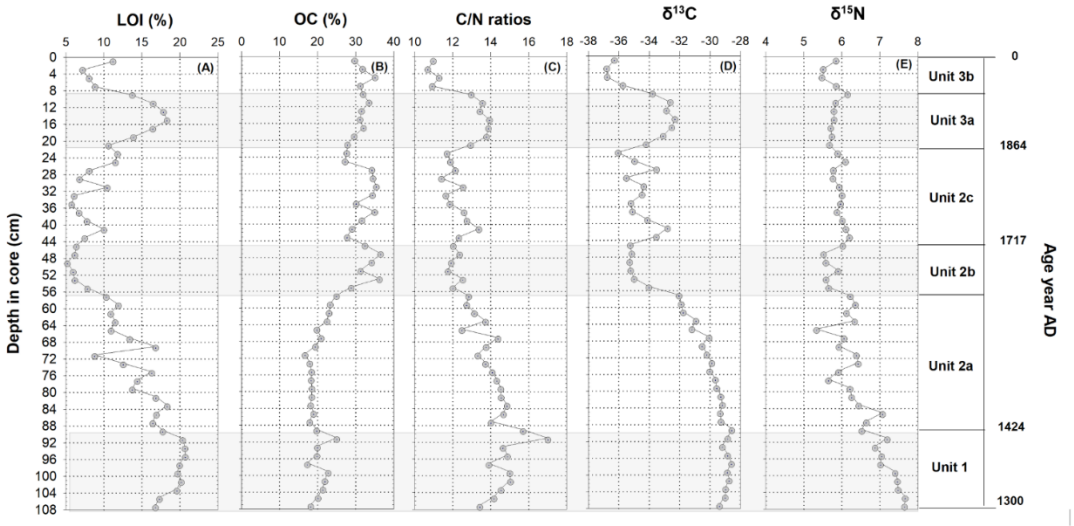

Figure 4.11. The variation of LOI (%), OC (%), C/N ratios, $\delta^{15}N$ and $\delta^{13}C$ in the sediment core with depth (cm)

$\delta^{13}C$ values varied from -28.57 to -36.8 ‰ with an average of -32.23±2 ‰. The data shows an inverse trend of the relationship between the $\delta^{13}C$ values and C/N ratios. Below the depth of 69 cm, $\delta^{13}C$ values had small fluctuations, then suddenly fell to a value of 34.99 ‰ at 53 cm in depth. From 53 to 23 cm, $\delta^{13}C$ values displayed a small variation, before increasing to the depth of 11 cm and then decreased to the surface sediment (Fig 4.11). $\delta^{15}N$ values slightly fluctuated from 5.33 to 7.67 ‰, with an average of 6.2±0.6 ‰ and can be separated into two-part. Below the depth of 47 cm, $\delta^{15}N$ values tended to gradually decrease, then showed a small values from 47 m to the surface sediment with the exception of samples near the surface (Fig 4.11).

LOI values is positively correlated with density of sediment, C/N ratio and $\delta^{13}C$ values follow by equations: Density (g/m^3) = 68.34*LOI - 37.3 (R^2=0.66), C/N ratios = 0.23*LOI + 10.25 (R^2 = 0.69), $\delta^{13}C$ = 0.45*LOI - 37.87 (R^2=0.66), respectively. Inversely, LOI values are negatively correlated with OC content, the linear regression line has an equation of the form TOC = -0.84*LOI + 36.83 (R^2=0.4), which means the sample with high of LOI values, as well as OC content was low.

Organic carbon (OC) content is positively correlated with organic nitrogen (Norg), the linear regression line has an equation of the form Norg = 0.1*OC-0.5 (R^2=0.94). The relationship between OC content and Norg suggested that organic carbon and total nitrogen in sediments mainly originated from organic matter. In contrast, OC content is negative correlated with C/N ratios and $\delta^{13}C$, follow by equations: C/N = -0.13OC+ 16.7 (R^2=0.69), $\delta^{13}C$=-0.36*OC-22.82 (R^2=0.75), respectively.

CHAPTER 5. RECONSTRUCTION OF PALEOENVIRONMENT AND PALEOCLIMATE IN NORTHERN VIETNAM AS INFERRED FROM SEDIMENTALOGICAL AND GEOCHEMICAL DATA

5.1. Reconstruction of Paleoenvironmental and Paleoclimate in Ao Tien Lake

According to Weide (2012), sedimentation rates in Ba Be lake was calculated by ^{14}C and ^{137}Cs dating in sediment core with the depth of 212 cm. This result shows the sedimentation rate in the bottom of the core (from 1.5 to 1.65 m in depth) is determined at 0.1 cm/year, from 1.3 to 1.4 m, the sedimentation rates increase to 0.2 cm/year and slightly increasing to 0.23 cm/year from 0.6-0.3 m (Weide, 2012). Moreover, the source of water in Ao Tien Lake exchanged with Ba Be Lake by the karst system. In core AT, the Mz values, sand contents, silt content had small fluctuations which suggested the source of sediment input from surrounding areas must be maintained in a stable condition/environment. In the present study, the average sedimentation rates in Ba Be lake below the depth of 0.13 m could represent for the Ao Tien lake's sedimentation rate, which means that the core length in Ao Tien corresponds to the last 700 years (from 1300 AD to present).

In unit 1 (from 108 to 90 cm), the Mz values and sand contents tended to slight decrease and inversely, mud contents tended to gradually increase. This pattern indicated that hydrological regimes are a favourable environment for fine-grain particles (Liu, et al., 2008). LOI values, C/N ratios and $\delta^{13}C$ had small fluctuations and they are the highest than other sections, indicating high lake water level and warmer climate (Yanhong, et al., 2006). LOI values and C/N ratios reached a maximum at the top sediment as 20.69 %, 17.01, respectively, suggesting a high amount of organic matter input at Ao Tien Lake. In addition, $\delta^{13}C$ values in this section were quite stable with an average of -28.9 ‰, indicating a large proportion of C3 plants in organic matter (Lamb, et al., 2007) (Fig 5.1). The core length in unit 1 corresponds to a period from 1300 to 1424 years AD. The record $\delta^{18}O$ measurements of stalagmite calcite in southern China (Dongge Cave) showed this period of high Asian monsoon intensity with a high precipitation, a decrease of $\delta^{18}O$ values (Dykoski, et al., 2005).

In unit 2 (from 90 to 23 cm), the sediment core could be classified into three parts. In the lowest part (from 90 to 57 cm), all LOI values, C/N ratios and $\delta^{13}C$, $\delta^{15}N$ tended to decrease with an average of 13.97±2.97 %, 13.92±0.85, -30.20 ±1.04 ‰ and 6.23±0.39 ‰, respectively. In addition, the parameters as Mz, So also tended to decrease but it is not clear. Sand contents suddenly decreased with an average of 15.74±2.96 %. Mz values tended to a slight decrease. So values were classified as poorly sorted sediment. In addition, the organic matter tended to change from high C3 plants to lake microalgae (Talbot&Lærdal, 2000). C/N ratios and $\delta^{13}C$ values tended to decrease which suggested that organic matter with a dominance of microalgae (Lamb, et al., 2007). $\delta^{15}N$ values tended to decrease suggested that a large proportion of microalgae/*cyanobacteria* and they can concentrate

nitrogen from the atmosphere for growing up, thus reducing $\delta^{15}N$ values in the sediment. The record $\delta^{18}O$ measurements of stalagmite calcite in southern China (Dongge Cave) and tree-ring base hydroclimate (reconstruction the Palmer Drought Severity Index - PDSI) showed this period of weak Asian monsoon intensity with a decrease of precipitation and variation in PDSI remained low (Buckley, et al., 2010, Dykoski, et al., 2005). In this period, the weakening of monsoonal activity in Northern Vietnam was supported by the percentage decrease in tropical rain forest and lake water level. In the middle part (from 57 to 45 cm), LOI values, C/N ratio, $\delta^{13}C$ values, and $\delta^{15}N$ varied over a small value and they tended to decrease. While the variation of mean grain size and sand content remained low. It is suggested that the enhanced microalgae biomass with a low level of water in Ao Tien Lake. The decreasing $\delta^{13}C$ and $\delta^{15}N$ values showed the dominance of *chrysophyceae* and cyanobacteria in lake microalgae. The results of, Dykoski *et al.,* (2005), Buckley *et al.,* (2010) also showed the decreasing precipitation in the first part, then continuously increased upward (Buckley, et al., 2010). Thus, the $\delta^{18}O$ values of stalagmite calcite in southern China (Dongge Cave) tended to decrease (Dykoski, et al., 2005). In the last part (from 45 to 23 cm), the parameters of sand contents, Mz values and So values tended to slightly increase. LOI values, $\delta^{13}C$ values, $\delta^{15}N$ values and C/N in this part tended to increase with an average of 8.23±2.58, -34.57±0.95 ‰, 5.97±0.13 ‰, and 12.18±0.56. This pattern suggested a high amount of sediment and organic matter into the lake from the surrounding area and the increase of organic matter derived from microalgae and C3 plants which grown up in the area surrounding. Thus, the lake water level was increased due to a high amount of water meteoric input at Ao Tien Lake. Otherwise, the enhanced Asian monsoon regime. These results were similar to those of the record $\delta^{18}O$ measurements of stalagmite calcite in southern China (Dongge Cave) (Dykoski, et al., 2005). At the end of this part, while the LOI values increased, C/N ratio and $\delta^{13}C$ decrease, a variation of $\delta^{15}N$ changed with time. The pattern indicated microalgae biomass developed with the high lake water level. At some point, $\delta^{13}C$ values increased, it can occur when ^{13}C content of inorganic carbon dissolved in water (Leng, et al., 2006). The core length in unit 2 corresponds to a period from 1424 to 1864 years AD.

In unit 3 (from 23 cm to the core surface), the sediment core can be divided into two distinguished part. In the lower part (from 23 to 9 cm), sand contents, Mz, So are strongly increased. While LOI values tended to slightly increase than the underlying part with an average of 15.31±2.73 %, C/N ratios and $\delta^{13}C$ also tended to gradually decrease with an average of 13.49±0.41 and -33.06±0.7 ‰. These results indicated the enhanced organic matter derived from C3 plants grown up in the area surrounding due to higher lake water level. The comparative with the record $\delta^{18}O$ measurements of stalagmite calcite in southern China (Dongge Cave) and tree-ring based

hydroclimate (reconstruction the PDSI) showed an increase of precipitation at the first of the part and slightly decrease at the end of this part (Buckley, et al., 2010, Dykoski, et al., 2005). In the upper part (from 9 to surface sediment core), sand contents, Mz values and So values markedly dropped with an average of Mz as 21.52±3.93 μm. Similarly, LOI values, C/N ratio, and $\delta^{15}N$ values tended to decrease upward. $\delta^{13}C$ values suddenly decreased and reached a minimum at 3 m in depth. This pattern indicated the decreasing amount of water input at Ao Tien Lake. Variation of $\delta^{13}C$ and C/N ratios remained low, suggesting the organic matter contents had derived from microalgae with a dominance of *chrysophyceae* (Lamb, et al., 2007, Vuorio, et al., 2006). The core length in unit 3 corresponds to a period from 1864 AD to present.

5.2. Recontruction of paleoenvironment and paleoclimate in the Red River Delta

5.2.1. Source of sediment organic matter

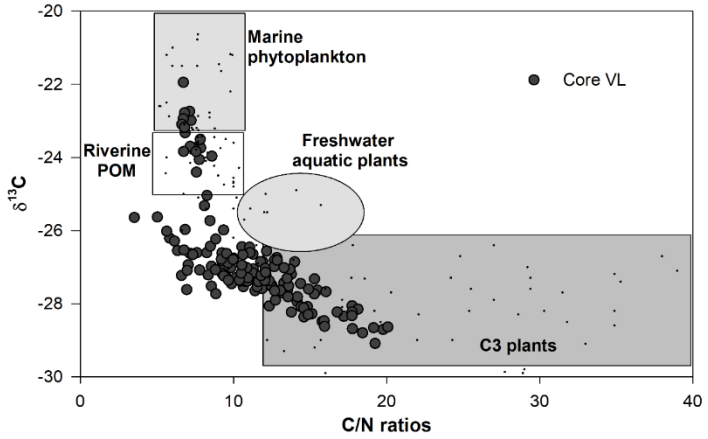

Figure 5.1. Bi-plot of $\delta^{13}C$ and C/N ratios for sediment core in the sediment core

Below at the depth of 30.1 m, this sediment section was characterized by low $\delta^{13}C$ values (< -27 ‰) and high C/N ratios (> 12), which showed that the sediment of this section was sourced from terrestrial vegetation (C3 plants) (Lamb, et al., 2007, Lamb, et al., 2006). Most notably, the variation of $\delta^{13}C$ value and C/N ratio at the erosion surface suggested the source of organic matter varied from terrestrial (C3 plants) to marine phytoplankton. The variation of $\delta^{13}C$ values and C/N ratios at the depth from 30.1 to 18.9 m suggested that the sedimentary organic matter was originated from marine phytoplankton, which located mainly in the lower layers of the sediment core and then gradually decreased. In which, in the part under (at the depth core between 30.1 and 26.3 m), the C/N ratios tended to increase and $\delta^{13}C$ values sharply dropped, which suggested that the dominant of the marine phytoplankton in the organic carbon source. In the part below (from 26.3 to 18.9 m in depth), the upward decreasing trends of $\delta^{13}C$ values and C/N ratios slightly increased, which investigated a decline of marine phytoplankton in the organic carbon source (Corner, et al., 1971, Liu, et al., 2007). In the core sediment section between 18.9 to 11.7 m, the variation of C/N ratios and $\delta^{13}C$ values

indicated a significant proportion of the sedimentary organic matter was originated from terrestrial C3 plants. In the last core sediment section from 11.7 m to core surface, $\delta^{13}C$ values slightly increase and C/N ratios gradually decreased, indicating a decline of terrestrial vegetation (C3 plants) in the organic carbon source, it could be caused by a increasing of particulate organic matter or freshwater aquatic plants in the estuary environment.

5.2.2. Source of clay minerals during the Holocene

In the study area, the multi-sourced clayey sediments derived from Song Hong catchment might have been well mixed in the marginal marine environment while the clays in the river discharge and floodplain better display their origin according to rapid transport sediment and accumulation. The appearance of gibbsite-kaolinite assemblage suggested not only a strong chemical weathering volume of supply source during the last glacial maximum but also fluvial activity of the regression stage in the wet and warm conditions (Li, et al., 2006). The concentration of smectite assemblage in sedimentary environments is controlled by sediment derivation from a different source terrain and also by grade (particle size) deposit. Because smectite remains in suspension, which transported further offshore for a long time. In addition, during the transportation process, the sediment could be carried detrital material from delta plain and passed into shallow marine. The abundance of Si ions in the sedimentary environment along the dry conditions could be leaded to the substitution of Al ions, which formed smectite-illite mixed layer and smectite materials. Inversely, heavy rainfall and strong chemical weathering along with warm/wet conditions, Si ions and other cations could be released and formed a large amount Kaolinite. However, in the marine environment illite could be leached to transform to smectite-illite mixed layer, smectite, which caused by the substitution of K^+ by Na^+(Meunier, 2005). Finally, the material is deposited in the marine environment during sedimentary transport (Chamley, 1989).

5.2.3. Sequence stratigraphy in the Red River Delta, Vietnam

Because the correlations of sedimentary characteristics between this study and the previously result by Tanabe et al., (2006) (VN core), the sedimentary facies and sequence stratigraphic of Holocene sediment were conducted following the longitudinal section C-D with three sediment cores VN, NB and GA (Tanabe, et al., 2006) (Fig 5.2). The Maximum Flooding Surface (MxFS) was investigated between estuarine sediments and deltaic sediment in the core (Fig 5.2). Below the MxFS, the deposition condition shows a deepening-upward succession. The deposition environment shifted from shelf to prodelta to delta plain. The MxFS in this study can be determined based on the occurrence of a shelly layer which overlies estuarine sediments with sharp erosion surface. According to a result by Tanabe et al., (2006), the erosional surface was eroded during a regression and the ages

of these shelly layers correspond 8.5 cal. kyr BP. As a result, Posamentier et al., (1988) investigated that the MxFS and the maximum paleo-water depth occur at the same time, but a time gap of about 1-5 kyr between the maximum paleo-water depth and MxFS which has been carried out in the Red River Delta (Lieu, 2006, Tanabe, et al., 2006).

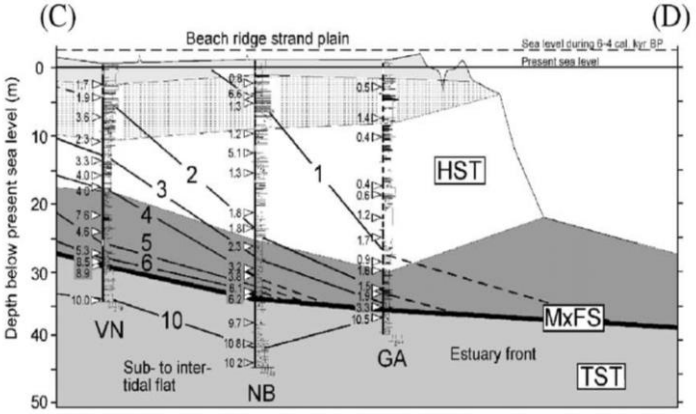

Figure 5.2. Sequence stratigraphic of the longitudinal section C-D in the RRD (cores VN, NB, GA) (after Tanabe et al., 2006)

The transgressive systems tract (TST) comprises dominance of retrogradational estuarine in the Red River Delta, including six sedimentary facies: tide-influenced channel-fill, lagoon, flood tidal delta, tidal flat, sub- to intertidal flat, estuary front sediments (Lieu, 2006, Tanabe, et al., 2006). In this study, the data show a TST interpretation of sub-to intertidal flat in the core of 36 - 30 m in depth and this facies is distributed and investigated in almost cores which published by Tanabe et al., (2006) and Lieu (2006) with an exception only to the HV core-site. The TST age is shifted from 8.5 to 15 cal. kyr. BP. The highstand systems tract (HST) comprises the dominance of progrdational deltaic sediments in the Red River Delta. The HTS corresponds to the duration of dropping sea level during the last phase of sea-level rose. In this period, sea-level changed from stable to dropping at the age of approximately 4-2 cal. kyr BP and the deltaic sediments prograded seaward (Fig 5.2).

5.2.4. Holocene evolution of the Red River Delta, Vietnam

During the state I, the sea-level was rising (Steinke, et al., 2003, Tanabe, et al., 2006). In this sate, the sea level in Vietnam was about 31 m below PSL and increased with a constant rate of about 9 mm per year (Tjallingii, et al., 2014). The color of the sediment (reddish-gray) showed erosion processes during low-stand of sea level. The sedimentary parameters illustrated a large portion of fine sand and coarse silt sediments, suggesting the dominance of sediment is originated in high-energy condition (McLaren&Bowles, 1985, Rajganapathi, et al., 2013). The upward increasing trends of C/N ratios (with an average 15.69) investigated that the dominant organic matter sourced from terrestrial vegetation (Lamb, et al., 2007, Tue, et al., 2011). In addition, $\delta^{13}C$ values fluctuated between

approximately -29 ‰ and -23 ‰ and it is similar to the result in the coastline of the RRD by Tue, et al., (2012), together indicating that the sedimentary organic carbon could be formed by mangroves forest (Tue, et al., 2012). Thus, this period could be defined as the sub- and intertidal environment which is strong controlled by tidal flooding (Li, et al., 2006, Tanabe, et al., 2006).

The state II has separated into two sub-state according to textural sediment, geochemical proxies and feature of lithology.

- In the lowest section, C/N ratios suddenly decreased and $\delta^{13}C$ values increased upward, together indicating that sedimentary organic carbon sources are quickly changed from terrestrial vegetation (C3 plants) to the dominance of marine phytoplankton (Lamb, et al., 2006, Wilson, et al., 2005). The sediment suggested as an erosional surface which has been formed along with the transgression (Tanabe, et al., 2003, Tanabe, et al., 2006, Tanaka, et al., 2011). In the period from 8.8 to 4.06 cal. kyr BP, the RRD was slightly submerged in the water surface caused by the rising of sea level (Tanabe, et al., 2006), leading to the depth water of sediment core (between 7 to 6 cal. kyr BP) located about 30 m lower than at present, caused by the acceleration of sea-level rise. This result is similar to the previous publish in RRD by Tanabe *et al.,* (2006). In addition, the upward increasing trends of Mz values (between 30.1 and 27.5 m in depth) investigated the erosion surface that has been overlain by sand sediment. C/N ratios decreased to the lowest value and $\delta^{13}C$ value increased to the maximal values, together suggesting the dominance of organic carbon formed by marine phytoplankton (Fig 5.3). The pattern only explained when the sediment is formed under the high sea level during the transgression period. It is similar to the previous studies, Tanaka *et al.,* (2011) were investigated a huge of marine ostracod records in the sediment core (VN) of the RRD. Results showed that the highest of sea-level was observed in the sediment layer at the depth between 28.7 and 26.7 m (about from 7.2 to 5.7 cal. kyr BP). A previous investigated that the sediment in this section formed under wave-dominated conditions by Tanaka *et al.,* (2011). The mean grain size and Sk values are varied in a small range at the depth between 26.7 and 18.7 m, indicating that the deposition environment with low hydrodynamic energy. This period is characterized by a dominance of mesokurtic and leptokurtic sediment which showed coarser-grained sizes are continuously deposited during transportation and tidal activities. C/N ratios tended to gradually increase upward and the small variation in $\delta^{13}C$ values, together indicating the sedimentary environment could be considered as a shelf-prodelta.

- In the upper section, the increasing trends of C/N ratios and $\delta^{13}C$ values shifted in a small range indicated that sedimentary organic carbon originated from diverse sources between terrestrial vegetation (C3 plants) and marine phytoplankton, or deposited from particulate organic matter. This

result shows the sediment facies of the RRD is higher affected by the fluvial sediment during this period (Duc, et al., 2007, Van Maren&Hoekstra, 2005). The sand fraction and Mz values tended to increase slightly at the depth between 18.7 and 11.7 m, showing that the hydrodynamic energy of this sub-state is higher than the lower layers (McLaren&Bowles, 1985). Skewness values varied from coarse to fine skewed sediment which indicated that the upward increasing trend of fine-grained particles, whilst, coarse-grained particle tended to decrease and a relatively high riverine input. The gradual change of textural sediment, feature of lithology and stable isotopes (C/N ratios, $\delta^{13}C$ values) in the underlying sediment facies, together suggesting that the sedimentary environment could be defined as delta front slope (Hori, et al., 2004, Li, et al., 2006).

In the state III, the sea-level tended to decrease to the present sea level. Notably, the sediment in the mouth has been formed shoals (Hori, et al., 2004, Li, et al., 2006). At the depth between 11.7 and 4.1 m (corresponded from 2.29 to 1.72 cal. kyr BP), the rate of sediment accumulation increased to the maximal value (1.94 cm each year) in this state (Li, et al., 2006, Tanabe, et al., 2003) and active progradation became dominant in the delta system (Li, et al., 2006, Mathers&Zalasiewicz, 1999). The increasing of the sand percentage, whilst, silt and clay percentages tended to decrease upward, together suggested that the coarser-grained size became predominated. Because they are concentrated in a shallower with low-energy condition and river-dominated which passed into the delta system. $\delta^{13}C$ values and C/N ratios varied in a large range which suggested that strongly interacted between C3 plants and particulate organic matter in the estuary (Fig 5.3). The sediment in this state was formed close to the paleo-estuary, consequently, the sedimentary environment corresponded to the delta front platform (Duc, et al., 2007, Tanabe, et al., 2006). According to the study by Van den Bergh *et al.,* (2007), this state corresponded with the depth lower than 10 m which located near estuary dunes. In addition, a study by Tanabe *et al.,* (2006) also investigated that the amount of sediment inputted to the delta system during the last 2 cal. kyr BP was higher than the sediment volume supplied from marine activities. In the depth from 4.1 to 0.5 m (corresponded from 1.72 to 0.55 cal. kyr BP), the increasing trends of clay fraction and mean grain size decreased upward, which suggested that the sediment was formed in low energy condition (Rajganapathi, et al., 2013). Moreover, C/N ratios (< 10) showed that the prevalence of particulate organic matter from sediment which was transported by tidal (Lamb, et al., 2007). While the variation of $\delta^{13}C$ suggested that C3 plants became predominated (Lamb, et al., 2007). The coordinated variation of both values above (C/N ratios and $\delta^{13}C$ values) was similar to the result reported by Wilson *et al.,* (2005) for tidal flat environment. Thus, the sedimentary environment of this core section corresponded to tidal a flat environment. At the depth from 0.5 to the surface core (corresponded from 0.55 cal. kyr BP to present), the lithological

characteristics were similar to a floodplain environment (in core VN) which reported by Tanabe *et al.*, (2006).

5.2.5. Clay mineralogy indicating the monsoon along the Holocene

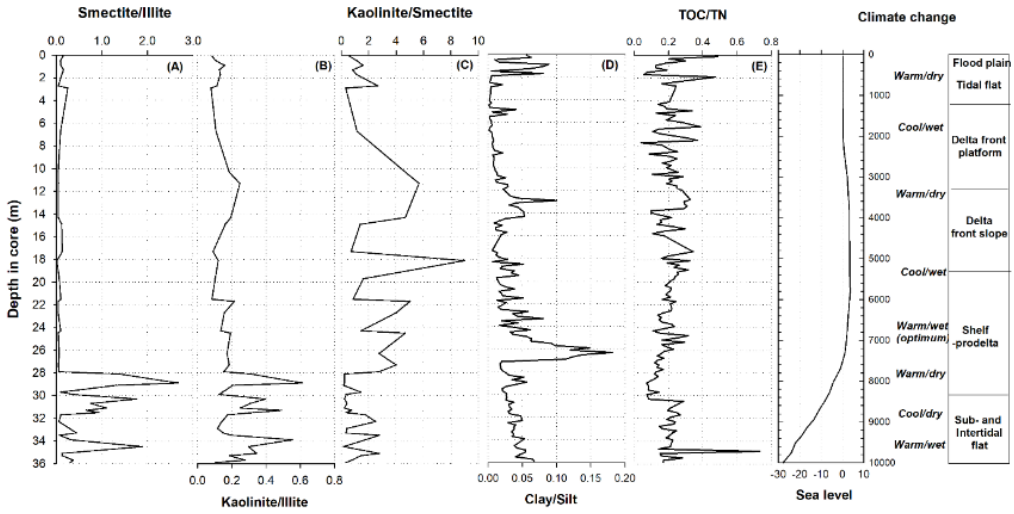

Figure 5.3. Variations in smectite/illite, kaolinite/illite and kaolinite/smectite ratios for the core from RRD. The clay/silt ratios, TOC/TN ratios and sea level are show for comparision

From 11.26 to 9.6 cal. kyr BP, the clay minerals component of this period is characterized mainly by kaolinite-rich than others. The kaolinite widely fluctuated and attained the highest values in this period which suggested that a slightly warmer climate than at present and enhanced chemical weathering. Organic geochemical data further imply that the paleoclimate was warmer than at present (Li, et al., 2006, Tanabe, et al., 2006). Based on pollen in the Changjiang, China, investing that the enhancing of East Asian Summer Monsoon with abundant rainfall and the dominance of chemical weathering along the early Holocene (Wang&Yang, 2013). Moreover, the clay fractions and C/N ratios were slightly higher and $\delta^{13}C$ values were the more negative, suggesting higher terrestrial carbon inputs or an increase in freshwater flux. This is supported by pollen records from the RRD indicating a warm and wet period due to the main from tropical pollens (Li, et al., 2006, Tue, et al., 2019).

During the period between 9.6 and 8.4 cal. kyr BP, the illite values tended to increase which caused by reducing rainfall and the dominance of physical weathering. The pollen and carbonate records from northeastern Cambodian lake sediment also showed the climate was cooler and drier than the present for at least 1000 years before 8.4 kyr ^{14}C years (about 9.3 cal. kyr BP) (Maxwell, 2001). The result similar to the reported from northeast Thailand, the cooler and dry period of about 9300-8.54 cal. kyr BP (Udomchoke, 1989). In addition, the acceleration of sea-level rise, the TOC and C/N ratios were low and $\delta^{13}C$ values markedly increased, suggesting that a decline in the

freshwater flux concerning the transgression process of seawater. Pollen records from core VN also investigating that the climate during this interval was dry and cold, as inferred from the percentage decrease in both tropical semi-evergreen forest and tropical rain forest (Fig 5.4f) and the dominance of temperate taxa (Li, et al., 2006). In this period, the marked increase in stalagmite $\delta^{18}O$ values from Dongge Cave (China) also indicated a dryer phase (Fig 5.4h) (Dykoski, et al., 2005).

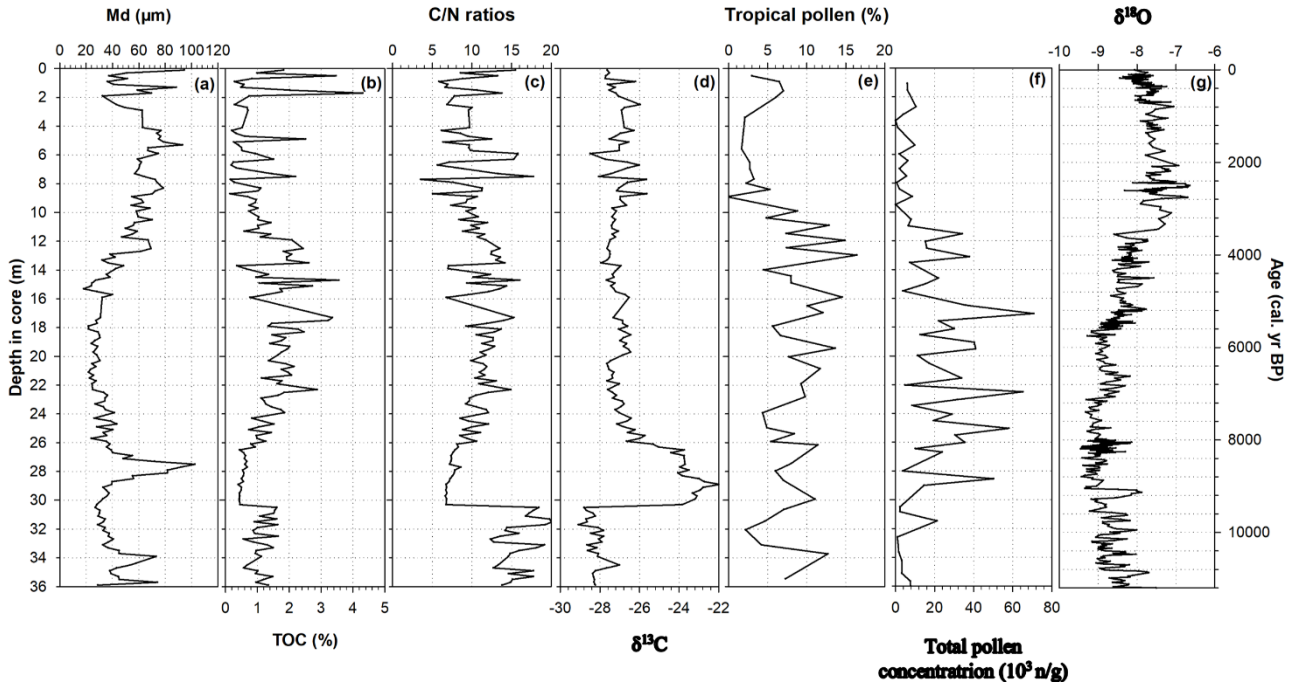

Figure 5.4. Comparison of the results from sediment core with other paleoclimate proxies. (a-d): Mean sediment grain sizes (Mz), TOC (%), C/N ratios and $\delta^{13}C$ analyzed in sediment core; (e-f): Tropical pollen proportions (%) and total pollen concentrations in sediment core VN (Li, Saito, Matsumoto, Wang, Tanabe, et al., 2006); (g) Spelepthem $\delta^{18}O$ record from Dongge Cave in southern China (Dykoski et al., 2005)

From 8.4 to 5.28 cal. kyr BP, the kaolinite values tended to increase, caused by enhancing of rainfall and the dominance of chemical weather. A large reduction of $\delta^{13}C$ values suggests that the maximum development of warm conditions and precipitation was reached at about 8 cal. kyr BP. In the Red River Delta, this period is considered as the Holocene climatic optimum with the high development of vegetation (Fig 5.4g) (Li, et al., 2006). The relatively high temperature and precipitation could be important factors intensifying erosion processes on land and transport the fine-grain size sediments to the Red River catchment. The study of the Hanjiang delta, southeast China also showed the warm climate during the middle Holocene, which began at 8.3 cal. kyr BP (Zheng&Li, 2000). Beside, Maxwell studied in northeastern Cambodia and showed conditions were relatively warm and moist during the period 8.4-5.3 cal. kyr BP (Maxwell, 2001).

Between 5.28 and 3.09 cal. kyr BP, the illite values tended to increase which caused by reducing rainfall and the dominance of physical weathering. The gradual increase in Mz values, the

high fluctuation of TOC and C/N ratios suggest that freshwater and organic matter fluxes from river systems may have declined. The weakening of monsoonal activity in this period was supported by pollen records which demonstrated a significant decline in the diversity of vegetation in the Red River Delta (Li, et al., 2006). Additionally, the slight increase in the stalagmite $\delta^{18}O$ values from Dongge Cave suggested a reduction of precipitation during this period (Dykoski, et al., 2005).

From 3.09 to 2.1 cal. kyr BP, a warm and dry climate is shown by the kaolinite and smectite values increased. Although kaolinite and smectite values show a slight decline after the depth of 11.3 m, however, a large portion of kaolinite and smectite in this period were higher than the lower part. The high abundance of tropical taxa of the core sediments VN also suggested similar paleoclimatic changes with warm climate (Li, et al., 2006).

Between 2.1 and 1.54 cal. kyr BP, the kaolinite contents tended to decrease which suggesting weaker chemical weathering and also the climate became cooler than at present. The increase in Mz and $\delta^{13}C$ values suggested a decrease in freshwater flux. This hypothesis is supported by the decrease in the percentage of tropical pollen species and total pollen concentration in core VN (Li, et al., 2006). The abrupt increase in the stalagmite $\delta^{18}O$ values from Dongge Cave (Dykoski, et al., 2005) also suggested the continuous weakening of the Asian monsoon intensity across the East Asia continent. Base on the regular variations of crystallographic indices in the core shows the decreasing of chemical weathering and monsoon precipitation during the late Holocene in the Changjiang Delta, China (Wang&Yang, 2013).

From 1.540 cal. kyr BP to present, a warming character is indicated by the kaolinite and smectite values increased and the dominance of chemical weathering. An increasing of freshwater flux is indicated by the decrease in $\delta^{13}C$. The clay mineral assemblages of the Chanjiang Delta also showed a weak monsoon precipitation along the late Holocene (Wang & Yang, 2013). Moreover, human activities are considered to affect on the natural vegetation. Rice cultivation was carried out in the RRD over the past 2000 to 3000 years (Oscar, 1995). After 1.54 cal. kyr BP, expansion of agricultural cultivation intensified as the climate became warm (Dykoski, et al., 2005).

CHAPTER 6. CONCLUSIONS

1. Climate change along the Holocene has been affected by natural factors and human activities (using fossil fuels deforestation, conversion of land use purpose,…). Climate viability along the Holocene in the World has been divided into three major periods: between 9-8 cal. kyr BP; classic "cool poles, dry tropics"; "cool poles, wet tropics" started at ~0.6 cal. kyr BP.

2. According to the results of pollen, ASM-^{14}C and facies study on two sediment core (VN and GA cores) from the RRD, the Holocene sea-level could be classified into the following three phases: from 9 to 6 cal. kyr BP (phase I); between 6 and 4 cal. kyr BP (phase II); from 4 to 0 cal. kyr BP (phase III).

3. The sediment in core AT could shows the changing paleoenvironments in Northern Vietnam during about 700 years. The variation of lithological characteristics, textural parameters (Mz, So, Sk, KG) and geochemical proxies (LOI, C/N ratio, δ^{13}C, δ^{15}N) suggested the sediment in core can be classified into three periods: unit 1 (from 108 to 90 cm); unit 2 (from 90 to 23 cm); unit 3 (from 23 to the core surface). Covariation of δ^{13}C, δ^{15}N and C/N ratios in the sediment core can be regarded to the organic carbon source, which showed from the dominant C3 plants (carbon fixation plants) surrounding lake at the unit 1 to both C3 plant and lake microalgae with a large proportion of chrysophyceae and cyanobacteria at the unit 2 and unit 3. Moreover, unit 3 was characterized by the dominance of chrysophyceae microalgae in the oligotrophic state.

The sediment core sample of the RRD can be classified into six deposition environments which consisted of sub-tidal flats and inter-tidal flats (from 36 to 30.1 m); shelf-prodelta (from 30.1 to 18.9 m); delta front slope (from 18.9-11.7 m); delta front platform (from 11.7 to 4.1 m), tidal flat (from 4.1 to 0.5 m) and flood plain (from 0.5 m to surface of sediment). The textural characteristics of the core sample were closely related to the core sample from the previous study in RRD. In a sediment core from 30.1 to 18.9 m, sediment showed erosion surface during the transgression at 8.86 cal. kyr BP. The textural parameter of the RRD has resulted in the interaction between sea-level shifts and fluvial inputs. In addition, the predominance of coarse silt very and coarse silt can be indicated the prevalence of comparatively from low to high energy conditions in the RRD.

Three cycles of warning and cooling were identified through isotopic analysis and clay mineral assosiation along the Holocene: a cool and wet climate during 9.6-8.4 cal. kyr BP, 5.28-3.09 cal. kyr BP, 2.1-1.54 cal. years BP and a warm climate during 11.260-9.6 cal. kyr BP, 8.4-5.28 cal. kyr BP, 3.09-2.1 cal. kyr BP and the present warm climate.

REFERENCES

Aaby, B.& Tauber, H., *1975. Rates of peat formation in relation to degree of humification and local environment, as shown by studies of a raised bog in Deninark. Boreas, 4 (1). 1-17.*

Aaby, B., *1976. Cyclic climatic variations in climate over the past 5,500 yr reflected in raised bogs. Nature, 263 (5575). 281.*

Battarbee, R. W.& Binney, H. A., *2009. Natural climate variability and global warming: a Holocene perspective. John Wiley & Sons.*

Berger, A., Mesinger, F.& Sijacki, D., *2012. Climate change: inferences from paleoclimate and regional aspects. Springer Science & Business Media.*

Biscaye, P. E., *1965. Mineralogy and sedimentation of recent deep-sea clay in the Atlantic Ocean and adjacent seas and oceans. Geological Society of America Bulletin, 76 (7). 803-832.*

Blott, S. J.& Pye, K., *2001. GRADISTAT: a grain size distribution and statistics package for the analysis of unconsolidated sediments. Earth surface processes and Landforms, 26 (11). 1237-1248.*

Brindley, G.& Gillery, F., *1956. X-ray identification of chlorite species. American Mineralogist: Journal of Earth and Planetary Materials, 41 (3-4). 169-186.*

Buckley, B. M., Anchukaitis, K. J., Penny, D., Fletcher, R., Cook, E. R., Sano, M., Wichienkeeo, A., Minh, T. T.& Hong, T. M., *2010. Climate as a contributing factor in the demise of Angkor, Cambodia. Proceedings of the National Academy of Sciences, 107 (15). 6748-6752.*

Chamley, H., *1989. Clay mineralogy.*

Corner, E. D. S., Davies, A. G., Frederick, S. R.& Maurice, Y., *1971. Plankton as a Factor in the Nitrogen and Phosphorus Cycles in the Sea. Advances in Marine Biology, Volume 9 101-204.*

Denton, G. H.& Karlén, W., *1973. Holocene climatic variations-their pattern and possible cause. Quaternary Research, 3 (2). 155-205.*

Duc, D. M., Nhuan, M. T., Van Ngoi, C., Nghi, T., Tien, D. M., van Weering, T. C.& van den Bergh, G., *2007. Sediment distribution and transport at the nearshore zone of the Red River delta, Northern Vietnam. Journal of Asian Earth Sciences, 29 (4). 558-565.*

Dykoski, C. A., Edwards, R. L., Cheng, H., Yuan, D., Cai, Y., Zhang, M., Lin, Y., Qing, J., An, Z.& Revenaugh, J., *2005. A high-resolution, absolute-dated Holocene and deglacial Asian monsoon record from Dongge Cave, China. Earth and Planetary Science Letters, 233 (1). 71-86.*

Fanning, D. S., Keramidas, V. Z.& El-Desoky, M. A., *1989. Micas. Minerals in soil environments, (mineralsinsoile). 551-634.*

Ha, N. T. T., Thao, N. T. P., Koike, K.& Nhuan, M. T., *2017. Selecting the Best Band Ratio to Estimate Chlorophyll-a Concentration in a Tropical Freshwater Lake Using Sentinel 2A Images from a Case Study of Lake Ba Be (Northern Vietnam). ISPRS International Journal of Geo-Information, 6 (9). 290.*

Hori, K., Tanabe, S., Saito, Y., Haruyama, S., Nguyen, V.& Kitamura, A., *2004. Delta initiation and Holocene sea-level change: example from the Song Hong (Red River) delta, Vietnam. Sedimentary Geology, 164 (3–4). 237-249.*

Hormes, A., Müller, B. U.& Schlüchter, C., *2001. The Alps with little ice: evidence for eight Holocene phases of reduced glacier extent in the Central Swiss Alps. The Holocene, 11 (3). 255-265.*

Jackson, M. L., *2005. Soil chemical analysis: advanced course. UW-Madison Libraries Parallel Press.*

Kunze, G.& Dixon, J. B., *1986. Pretreatment for mineralogical analysis. Methods of Soil Analysis: Part 1—Physical and Mineralogical Methods, (methodsofsoilan1). 91-100.*

Lamb, A. L., Wilson, G. P.& Leng, M. J., *2006. A review of coastal palaeoclimate and relative sea-level reconstructions using δ13C and C/N ratios in organic material. Earth-Science Reviews, 75 (1-4). 29-57.*

Lamb, A. L., Vane, C. H., Wilson, G. P., Rees, J. G.& Moss-Hayes, V. L., *2007. Assessing $\delta^{13}C$ and C/N ratios from organic material in archived cores as Holocene sea level and palaeoenvironmental indicators in the Humber Estuary, UK. Marine Geology, 244 (1-4). 109-128.*

Leng, M. J., Lamb, A. L., Heaton, T. H., Marshall, J. D., Wolfe, B. B., Jones, M. D., Holmes, J. A.& Arrowsmith, C., *2006. Isotopes in lake sediments. Springer.*

Li, Z., Saito, Y., Matsumoto, E., Wang, Y., Haruyama, S.& Hori, K., *2006. Palynological record of climate change during the last deglaciation from the Song Hong (Red River) delta, Vietnam. Palaeogeography, Palaeoclimatology, Palaeoecology, 235 (4). 406-430.*

Li, Z., Saito, Y., Matsumoto, E., Wang, Y., Tanabe, S.& Lan Vu, Q., *2006. Climate change and human impact on the Song Hong (Red River) Delta, Vietnam, during the Holocene. Quaternary International, 144 (1). 4-28.*

Lieu, N. T. H., *2006. Holocene evolution of the central Red River Delta, Northern Vietnam lithological and mineralogial investigations. PhD thesis, Greifswald University, Germany.*

Liu, K.-K., Kao, S.-J., Hu, H.-C., Chou, W.-C., Hung, G.-W.& Tseng, C.-M., *2007. Carbon isotopic composition of suspended and sinking particulate organic matter in the northern South China Sea—from production to deposition. Deep Sea Research Part II: Topical Studies in Oceanography, 54 (14-15). 1504-1527.*

Liu, X., Herzschuh, U., Shen, J., Jiang, Q.& Xiao, X., *2008. Holocene environmental and climatic changes inferred from Wulungu Lake in northern Xinjiang, China. Quaternary Research, 70 (3). 412-425.*

Mackay, A., Battarbee, R., Birks, J.& Oldfield, F., *2003. Global change in the Holocene. Arnold, Hodder Headline Group.*

Martin, R. E., Leorri, E.& McLaughlin, P. P., *2007. Holocene sea level and climate change in the Black Sea: multiple marine incursions related to freshwater discharge events. Quaternary International, 167 61-72.*

Mathers, S., Davies, J., McDonald, A., Zalasiewicz, J.& Marsh, S., *1996. The Red River delta of Vietnam. British Geological Survey Technical Report WC/96/02,*

Mathers, S.& Zalasiewicz, J., *1999. Holocene sedimentary architecture of the Red River delta, Vietnam. Journal of Coastal Research, 314-325.*

Maxwell, A. L., *2001. Holocene monsoon changes inferred from lake sediment pollen and carbonate records, northeastern Cambodia. Quaternary Research, 56 (3). 390-400.*

Mayewski, P. A., Meeker, L. D., Twickler, M. S., Whitlow, S., Yang, Q., Lyons, W. B.& Prentice, M., *1997. Major features and forcing of high-latitude northern hemisphere atmospheric circulation using a 110,000-year-long glaciochemical series. Journal of Geophysical Research: Oceans, 102 (C12). 26345-26366.*

Mayewski, P. A., Rohling, E. E., Curt Stager, J., Karlén, W., Maasch, K. A., David Meeker, L., Meyerson, E. A., Gasse, F., van Kreveld, S., Holmgren, K., Lee-Thorp, J., Rosqvist, G., Rack, F., Staubwasser, M., Schneider, R. R.& Steig, E. J., *2004. Holocene climate variability. Quaternary Research, 62 (3). 243-255.*

McLaren, P.& Bowles, D., *1985. The effects of sediment transport on grain-size distributions. Journal of Sedimentary Research, 55 (4). 457-470.*

Meunier, A., *2005. Clays. Springer Science & Business Media,*

Milliman, J. D.& Syvitski, J. P., *1992. Geomorphic/tectonic control of sediment discharge to the ocean: the importance of small mountainous rivers. The journal of Geology, 100 (5). 525-544.*

Milliman, J. D., *1995. River discharge to the sea: a global river index (GLORI). LOICZ reports and studies, 2.*

Moore, D.& Reynolds Jr, R., *1997. X-ray Diffraction and the Identification and Analysis of Clay Minerals.*

Müller, A.& Mathesius, U., *1999. The palaeoenvironments of coastal lagoons in the southern Baltic Sea, I. The application of sedimentary Corg/N ratios as source indicators of organic matter. Palaeogeography, Palaeoclimatology, Palaeoecology, 145 (1-3). 1-16.*

Nghi, T., Toan, N. Q., Minh, N. D.& Van Vuong, N., *1991. Quaternary sedimentation of the principal deltas of Vietnam. Journal of Southeast Asian Earth Sciences, 6 (2). 103-110.*

Oscar, C., *1995. A History of Vietnam: From Hong Bang to Tu Duc.*

Poppe, L., Paskevich, V., Hathaway, J.& Blackwood, D., *2001. A laboratory manual for X-ray powder diffraction. US Geological Survey Open-File Report, 1 (041). 1-88.*

Pruszak, Z., Van Ninh, P., Szmytkiewicz, M., Hung, N. M.& Ostrowski, R., *2005. Hydrology and morphology of two river mouth regions (temperate Vistula Delta and subtropical Red River Delta). Oceanologia, 47 (3).*

Rabenhorst, M., Wilding, L.& West, L., *1984. Identification of Pedogenic Carbonates using Stable Carbon Isotope and Microfabric Analyses 1. Soil Science Society of America Journal, 48 (1). 125-132.*

Rajganapathi, V., Jitheshkumar, N., Sundararajan, M., Bhat, K.& Velusamy, S., *2013. Grain size analysis and characterization of sedimentary environment along Thiruchendur coast, Tamilnadu, India. Arabian Journal of Geosciences, 6 (12). 4717-4728.*

Rind, D., *2002. The Sun's role in climate variations. Science, 296 (5568). 673-677.*

Rohling, E., Mayewski, P., Abu-Zied, R., Casford, J.& Hayes, A., *2002. Holocene atmosphere-ocean interactions: records from Greenland and the Aegean Sea. Climate Dynamics, 18 (7). 587-593.*

Scuderi, L. A., *1993. A 2000-year tree ring record of annual temperatures in the Sierra Nevada mountains. Science, 259 (5100). 1433-1436.*

Starkey, H. C., Blackmon, P. D.& Hauff, P. L., *1984. The routine mineralogical analysis of clay-bearing samples. Geological Survey bulletin (USA). no. 1563.*

Steinke, S., Kienast, M.& Hanebuth, T., *2003. On the significance of sea-level variations and shelf paleo-morphology in governing sedimentation in the southern South China Sea during the last deglaciation. Marine Geology, 201 (1-3). 179-206.*

Talbot, M. R.& Lærdal, T., *2000. The Late Pleistocene-Holocene palaeolimnology of Lake Victoria, East Africa, based upon elemental and isotopic analyses of sedimentary organic matter. Journal of Paleolimnology, 23 (2). 141-164.*

Tanabe, S., Hori, K., Saito, Y., Haruyama, S., Vu, V. P.& Kitamura, A., *2003. Song Hong (Red River) delta evolution related to millennium-scale Holocene sea-level changes. Quaternary Science Reviews, 22 (21–22). 2345-2361.*

Tanabe, S., Saito, Y., Lan Vu, Q., Hanebuth, T. J. J., Lan Ngo, Q.& Kitamura, A., *2006. Holocene evolution of the Song Hong (Red River) delta system, northern Vietnam. Sedimentary Geology, 187 (1–2). 29-61.*

Tanaka, G., Komatsu, T., Saito, Y., Nguyen, D. P.& Vu, Q. L., *2011. Temporal changes in ostracod assemblages during the past 10,000 years associated with the evolution of the Red River delta system, northeastern Vietnam. Marine Micropaleontology, 81 (3). 77-87.*

Tjallingii, R., Stattegger, K., Stocchi, P., Saito, Y.& Wetzel, A., *2014. Rapid flooding of the southern Vietnam shelf during the early to mid-Holocene. Journal of Quaternary Science, 29 (6). 581-588.*

Tran, M.& Nguyen, V. D., *1991. Groundwater resources in Hanoi area. Geological survey of Vietnam,*

Tue, N. T., Hamaoka, H., Sogabe, A., Quy, T. D., Nhuan, M. T.& Omori, K., *2011. The application of $\delta^{13}C$ and C/N ratios as indicators of organic carbon sources and paleoenvironmental change of the mangrove ecosystem from Ba Lat Estuary, Red River, Vietnam. Environmental Earth Sciences, 64 (5). 1475-1486.*

Tue, N. T., Ngoc, N. T., Quy, T. D., Hamaoka, H., Nhuan, M. T.& Omori, K., *2012. A cross-system analysis of sedimentary organic carbon in the mangrove ecosystems of Xuan Thuy National Park, Vietnam. Journal of sea research, 67 (1). 69-76.*

Tue, N. T., Dung, L. V., Nhuan, M. T.& Omori, K., *2014. Carbon storage of a tropical mangrove forest in Mui Ca Mau National Park, Vietnam. Catena, 121 119-126.*

Tue, N. T., Quan, D. M., Nguyen, P. T., Dung, L. V., Quy, T. D.& Nhuan, M. T., *2019. Holocene environmental changes in Red River delta, Vietnam as inferred from the stable carbon isotopes and C/N ratios. Journal of Earth System Science, 128 (1). 15.*

Udomchoke, V., *1989. Quaternary stratigraphy of the Khorat Plateau area, northeastern Thailand. Proceedings of the Workshop on Correlation of Quaternary Successions in South, East and Southeast Asia, 69-94.*

Van Maren, D.& Hoekstra, P., *2005. Dispersal of suspended sediments in the turbid and highly stratified Red River plume. Continental Shelf Research, 25 (4). 503-519.*

Vuorio, K., Meili, M.& Sarvala, J., *2006. Taxon-specific variation in the stable isotopic signatures ($\delta^{13}C$ and δ15N) of lake phytoplankton. Freshwater biology, 51 (5). 807-822.*

Wang, Q.& Yang, S., *2013. Clay mineralogy indicates the Holocene monsoon climate in the Changjiang (Yangtze River) Catchment, China. Applied Clay Science, 74 28-36.*

Weide, D. M., *2012. Freshwater diatoms as a proxy for Late Holocene monsoon intensity in Lac Ba Be in the Karst Region of Northern Viet Nam. California State University (Thesis).*

Wilson, G. P., Lamb, A. L., Leng, M. J., Gonzalez, S.& Huddart, D., *2005. δ13C and C/N as potential coastal palaeoenvironmental indicators in the Mersey Estuary, UK. Quaternary Science Reviews, 24 (18-19). 2015-2029.*

Wright, H. E., *1993. Global climates since the last glacial maximum. U of Minnesota Press,*

Yanhong, W., Lücke, A., Zhangdong, J., Sumin, W., Schleser, G. H., Battarbee, R. W.& Weilan, X., *2006. Holocene climate development on the central Tibetan Plateau: a sedimentary record from Cuoe Lake. Palaeogeography, Palaeoclimatology, Palaeoecology, 234 (2). 328-340.*

Zheng, Z.& Li, Q., *2000. Vegetation, climate, and sea level in the past 55,000 years, Hanjiang Delta, Southeastern China. Quaternary Research, 53 (3). 330-340.*